REPORT DOCUMENTATION PAGE

Form Approved OMB No. 0704-0188

1. AGENCY USE ONLY (Leave blank)	2. REPORT DATE	3. REPORT TYPE AND DATES COVERED
	August 2002	Final Technical Report

4. TITLE AND SUBTITLE

Controllable Wheeled Vehicle Suspension Research

5. FUNDING NUMBERS

C-N68171-01-M-5852

6. AUTHOR(S)

Prof. N.J. Theron, P.S. Els

7. PERFORMING ORGANIZATION NAME(S) AND ADDRESS(ES)

Research Enterprises, University of Pretoria , PO Box 14679, Hatfield 0028, South Africa

M0016

9. SPONSORING/MONITORING AGENCY NAME(S) AND ADDRESS(ES

US Naval Regional Contracting Center Detachment London, Government Buildings, Block 2, Wing 12

U.S. Army Tank-Automotive Command, ATTN: Dr. F. Hoogterp, Warren, MI 48397-50000

10. SPONSORING/MONITORING AGENCY REPORT NUMBER

R&D 9086-AN-01S

11. SUPPLEMENTARY NOTES

Final Technical Report for contract no. N68171-00-M-5852, 52 pages.

12a. DISTRIBUTION/AVAILABILITY STATEMENT

Approved for Public Release.

12b. DISTRIBUTION CODE

A

ABSTRACT (Maximum 200 words)

The classic compromise between wheeled vehicle ride comfort and handling is well known. For off-road vehicles (as used by the military), it is very difficult to achieve a good compromise due to the fact that these vehicles are used on highways at high speeds. Controllable suspension systems offer the possibility to change the spring and damper characteristics while the vehicle is moving, thereby adapting to different terrains and speeds. This research involved the design, development, manufacturing, modeling and testing of a two-stage, semi-active, hydro-pneumatic spring, combined with a two stage semi-active damper. This system promises to improve both the ride comfort and handling (and therefore the mobility) of military wheeled vehicles. Test results indicate that the required characteristics can be achieved, and a design study proves the feasibility of fitting the system to a vehicle. It is concluded that the proposed suspension system is feasible and that further development of the system should continue.

14. SUBJECT TERMS

US Army Research, South Africa, Wheeled vehicle, Suspension, Control, Semi-active, Vehicle Dynamics, Simulation, Hydropneumatic, Ride comfort, Handling

15. NUMBER OF PAGES

16. PRICE CODE

17. SECURITY CLASSIFICATION OF REPORT	18. SECURITY CLASSIFICATION OF THIS PAGE	19. SECURITY CLASSIFICATION OF ABSTRACT	20. LIMITATION OF ABSTRACT
Unclassified	Unclassified	Unclassified	Unlimited

AD

Controllable Wheeled Vehicle Suspension Research

Final Technical Report
by

Prof. N.J. Theron, Mr. P.S. Els
August 2002

United States Army

EUROPEAN RESEARCH OFFICE OF THE U.S. ARMY

London, England

CONTRACT NUMBER : N68171-01-M-5852

R&D 9056-AN-01S

Research Enterprises at University of Pretoria (PTY) LTD

SOUTH AFRICA

Abstract

The classic compromise between wheeled vehicle ride comfort and handling is well known. For off-road vehicles (as used by the military), it is very difficult to achieve a good compromise due to the fact that these vehicles are also used on highways at high speeds. Controllable suspension systems offer the possibility to change the spring and damper characteristics while the vehicle is moving, thereby adapting to different terrains and speeds. This research involved the design, development, manufacturing, modeling and testing of a two-stage, semi-active, hydro-pneumatic spring, combined with a two stage semi-active damper. This system promises to improve both the ride comfort and handling (and therefore the mobility) of military wheeled vehicles. Test results indicate that the required characteristics can be achieved, and a design study proves the feasibility of fitting the system to a vehicle. It is concluded that the proposed suspension system is feasible and that further development of the system should continue.

List of Keywords

Wheeled vehicle
Suspension
Control
Semi-active
Vehicle Dynamics Simulation
Hydropneumatic
Spring
Damper
Ride comfort
Handling

Table of Contents

List of Appendixes

1. Statement of problem

The design of wheeled vehicle suspension systems always involved a compromise between ride comfort and handling. For good ride comfort a compliant suspension system is normally required while good handling demands a stiff suspension system to control body roll. With a normal passive suspension system, the characteristics of the springs and dampers are fixed at the design stage and cannot be changed afterwards. By using controllable springs and dampers, these characteristics can be changed while the vehicle is moving. It therefore becomes possible to have soft settings for good ride comfort whilst traveling in a straight line on a good road, while the suspension can be changed to a hard setting moments later to give good handling when the vehicle has to change direction as required for lane changing or even accident avoidance. Controllable suspension systems can therefore reduce or even eliminate the ride comfort vs. handling compromise.

2. Background to problem

The South African controllable suspension research effort over the last twelve years concentrated on semi-active dampers and hydro-pneumatic springs for wheeled off-road vehicles. An overview of all the research activities during this period can be found in references [1] to [18].

The Tank Automotive Command (TACOM) of the US Army's research activities focused on semi-active as well as fully active suspension systems. This included the development of an electric active suspension actuator and fully active hydraulic suspension for a high mobility off-road wheeled vehicle. TACOM experience is based on test results for both wheeled and track vehicles.

Experience in South Africa correlates very well with US experience and the lessons learned and conclusions reached are in good agreement. Improvements are in the same order of magnitude and problems identified with current semi-active suspension systems are also very similar. A similar approach to advanced suspension research is followed in that, although mathematical analysis and simulation is performed, the validation of results is obtained during field tests with suspension hardware fitted to vehicles and tested under real life conditions.

During discussions between Mr. P.S. Els (University of Pretoria, South Africa) and Dr. F.B. Hoogterp (TACOM, Detroit) in September 2000 [19], a definite mutual research interest in the field of semi-active suspension systems was identified. The idea of adding a semi-active hydro-pneumatic spring to the semi-active damper technology, as proposed by Els [2], is novel and warrants more detailed investigation. The resulting research project is defined in [20].

3. Approach to solving problem

The purpose of this research is to design, develop, manufacture and test a two-stage, semi-active, hydropneumatic spring, combined with a two stage semi-active damper. The resulting suspension hardware is tested and characterized to obtain all the parameters required for mathematical modeling. In order to investigate the feasibility of the proposed suspension system, the project included six tasks namely :

i) Developing a basic vehicle dynamics simulation model to predict ride comfort and handling.
ii) Determining the required suspension characteristics for the "best" ride comfort and "best" handling respectively, using the vehicle dynamics model.
iii) Designing a prototype suspension system capable of producing the required characteristics.
iv) Manufacturing the prototype suspension system according to the design.
v) Testing and characterisation of the prototype suspension system to determine feasibility and conformance to specification.
vi) Developing a mathematical model of the prototype suspension system that can be incorporated into the vehicle dynamics model at a later stage.

These six tasks will now be described in more detail.

3.1. Basic vehicle dynamics simulation model

In order to simulate the ride comfort and handling of a vehicle, simulation models, based on parameters for a Landrover Defender 110 sports utility vehicle (see figure 1), were developed in DADS (Dynamic Analysis and Design System) and MATLAB respectively.

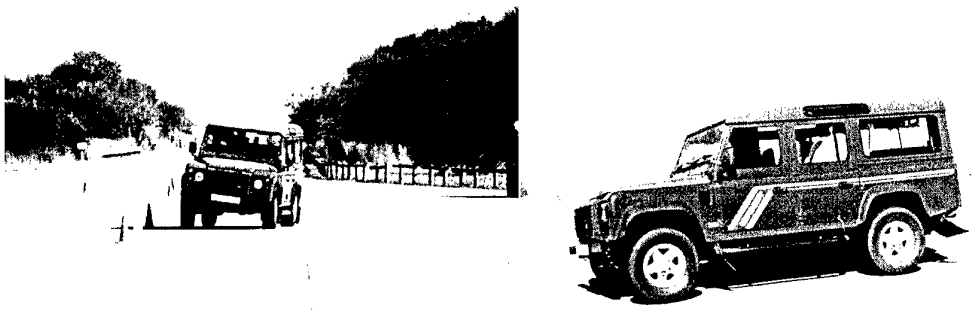

Figure 1 – Landrover Defender 110 vehicle

The DADS model has 81 degrees of freedom, but after adding joints, constraints and a driver model, 14 unconstrained degrees of freedom remain. These consist of the vehicle body displacements (lateral, longitudinal, vertical, roll, pitch and yaw), wheel rotations, front axle vertical displacement and roll and rear axle vertical displacement and roll. Non-linear spring, damper, bump stop and tire characteristics are used. The vehicle is steered over a predetermined course by a simple driver model which estimates the lateral positional error based on the yaw angle of the vehicle body at the current time step and the desired lateral position at a specified driver preview time. The driver model is implemented using amplifiers, summers and input elements. The basic components of the DADS model are summarized in table 1.

A simple dynamic model for simulating the ride response of the Landrover Defender 110 sport utility vehicle was also developed and coded in MATLAB. At the time when this was done the comprehensive model of the vehicle, including the suspension system geometry and kinematics, was already running successfully within the DADS (Dynamic Analysis and Design System) environment.

Model entities	Components	Quantity
Rigid bodies (13)	Vehicle body	2
	Wheels	4
	Front axle	1
	Rear axle	1
	Ground (fixed in space)	1
	Front hubs (left & right)	2
	Anti-rollbars	2
Revolute joints (9)	Front wheels to front hubs	2
	Front hubs to front axle	2
	Rear wheels to rear axle	2
	Body torsional stiffness	1
	Anti-rollbar left and right	2
Spherical-spherical joints (5)	Axle locating and push-pull rods, steering links	5
Revolute-revolute joint (1)	Radius rod	1
Revolute-spherical joints (2)	A-arm rear	1
	Panhard rod front	1
Constraints (2)	Steering control input	1
	Forward speed	1
Force elements (18)	Non-linear dampers	4
	Springs (choice of hydropneumatic and coil springs)	4
	Bump stops	4
	Generic tires	4
	Body torsional stiffness spring	1
	Anti-rollbar stiffness	1
Control elements (9)	Amplifiers	2
	Summers	2
	Inputs	2
	Steering angle limiter	1
	Output torques left and right	2
Initial conditions (1)	Vehicle forward speed	1

Table 1 - Components of the DADS model

The purpose of the MATLAB model was not to replace the DADS model. It was assumed that such a code, based on simple and fairly rough approximations to the suspension kinematics and limited to only small angle rotations (i.e., excluding yaw and thus steering, handling and any lateral dynamics) and with a very simple point contact tire model would execute significantly faster than the full DADS model. The plan was to use this code in the design of the control system of the semi-active suspension system, with special emphasis on the vehicle ride. In addition to the expected quicker execution speed, a second reason for developing the MATLAB code was that, at the

time, only one license to DADS was available (as opposed to a number of licenses to the ADAMS program, acquired recently). Having available an additional dynamic model of the vehicle was deemed beneficial in freeing the single DADS license for other work while the ride characteristics of the semi-active suspension system was investigated.

The MATLAB code is based on the equations of motion of the vehicle system. The derivation of these equations using Lagrangean dynamics is shown in Appendix A.

The simulation results of the MATLAB code compares well with simulation results predicted by DADS. A number of figures comparing outputs from the two programs for the same excitation condition are included below.

Simulations of the Landrover Defender 110 being driven at a constant speed of 60 km/h over a stretch of rough road identified as "Belgian paving" were done with both models. Figure 2 shows the comparison of the vertical displacement of the vehicle body center of gravity, as predicted by the two models. The comparison is generally fairly good. The second derivative of this data, presented in figure 3 as the vertical acceleration of the vehicle body center of gravity clearly shows that the DADS model predicted significantly more high frequency activity than the MATLAB model. This may be due to the fact that the DADS model has a larger number of degrees of freedom, giving rise to high frequency modes. The DADS model also fairly accurately accounts for the suspension kinematics and it is expected that modeling the kinematics will also give rise to high frequency behavior. Comparisons of the results predicted by the two models with respect to the front axle vertical displacement and the body roll angle are included in figures 4 and 5. These figures confirm that the two models generally agree well but that the DADS model predicts high frequency activity that is missed by the MATLAB model.

To investigate more specifically body roll dynamics of the MATLAB model, simulations were performed of the Landrover being driven with only its left hand side wheels over a 150 mm high 300 mm wide platform-like obstacle with straight up and down ramps at 11.3°. The right hand side wheels followed a flat road surface. This obstacle is locally referred to as the APG obstacle. The MATLAB model indicated that if this obstacle is crossed over at 10 km/h the bump stops hit through, in which case the simulation is terminated since it does not allow extrapolation on graphs. The DADS model may also indicate this, but it was not specifically investigated. The DADS model does not necessarily terminate, though, at such an occurrence.

Because of the MATLAB termination problems the simulation was done at a slow 5 km/h. The vehicle body center of gravity vertical displacement and roll angle results are compared in figures 6 and 7. The comparison between the MATLAB and DADS models are generally good.

These results show that the MATLAB code is performing in an acceptable manner and may be used in future for the design of the control system, with respect to vehicle ride, under conditions of small angles of roll and pitch.

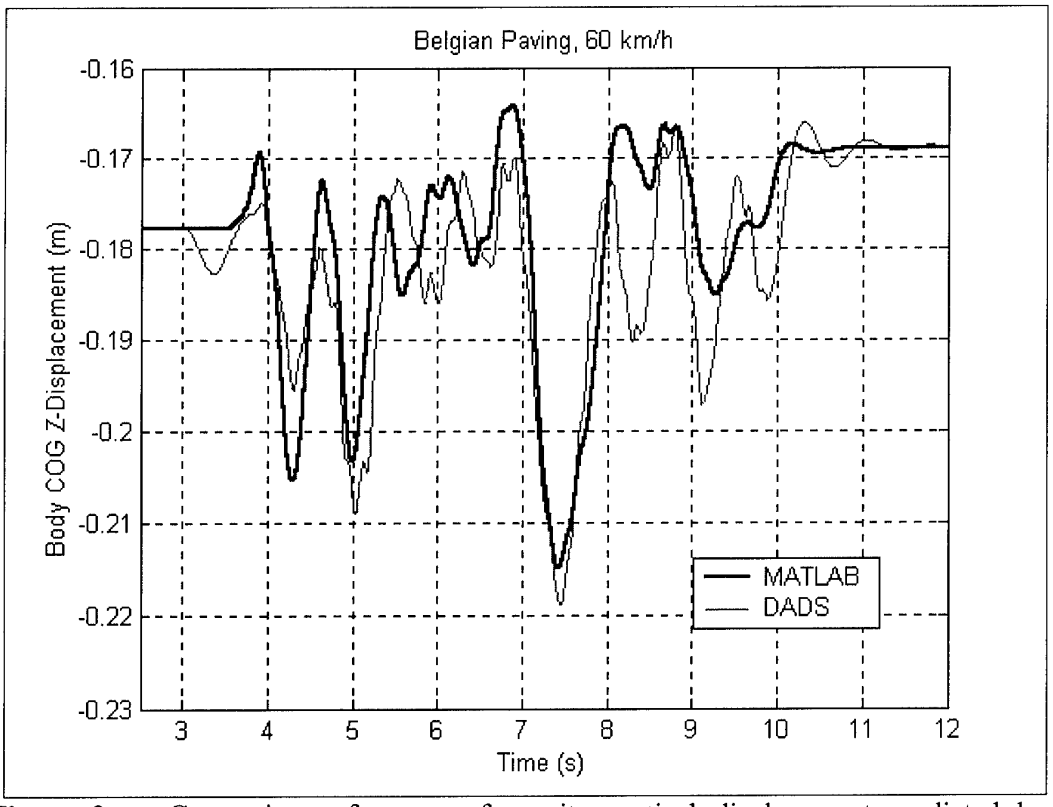

Figure 2 - Comparison of center of gravity vertical displacement predicted by MATLAB and DADS models for a Belgian paving road traversed at 60 km/h.

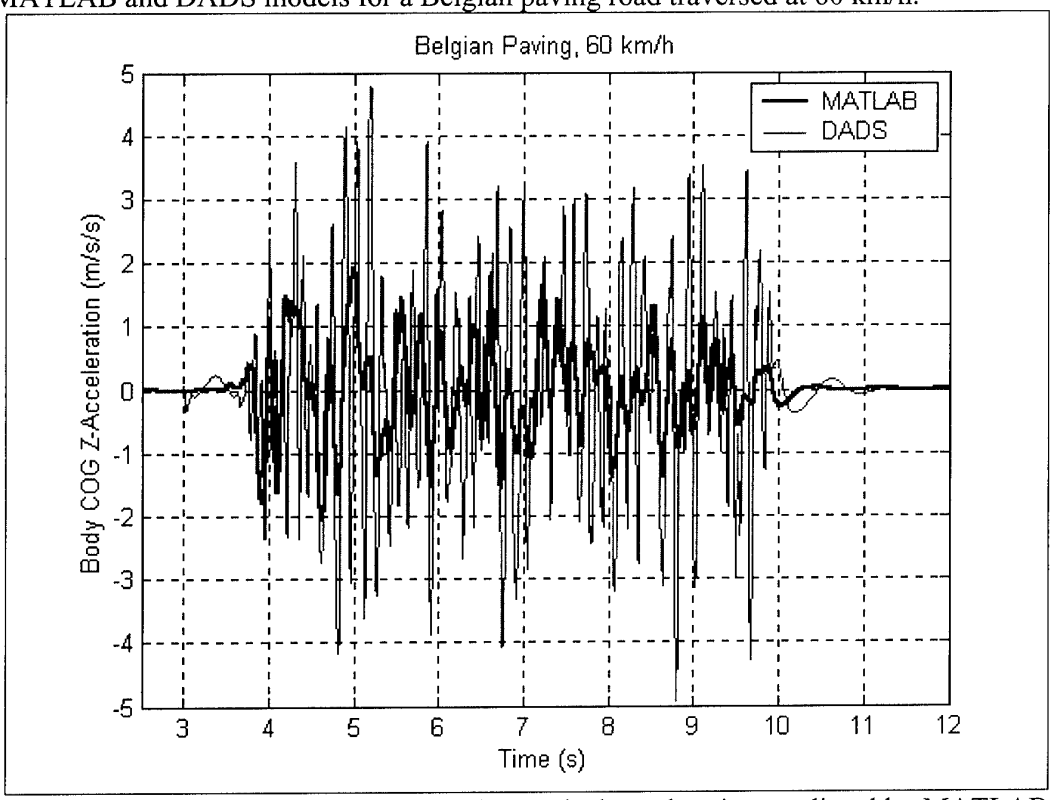

Figure 3 - Comparison of center of gravity vertical acceleration predicted by MATLAB and DADS models for a Belgian paving road traversed at 60 km/h.

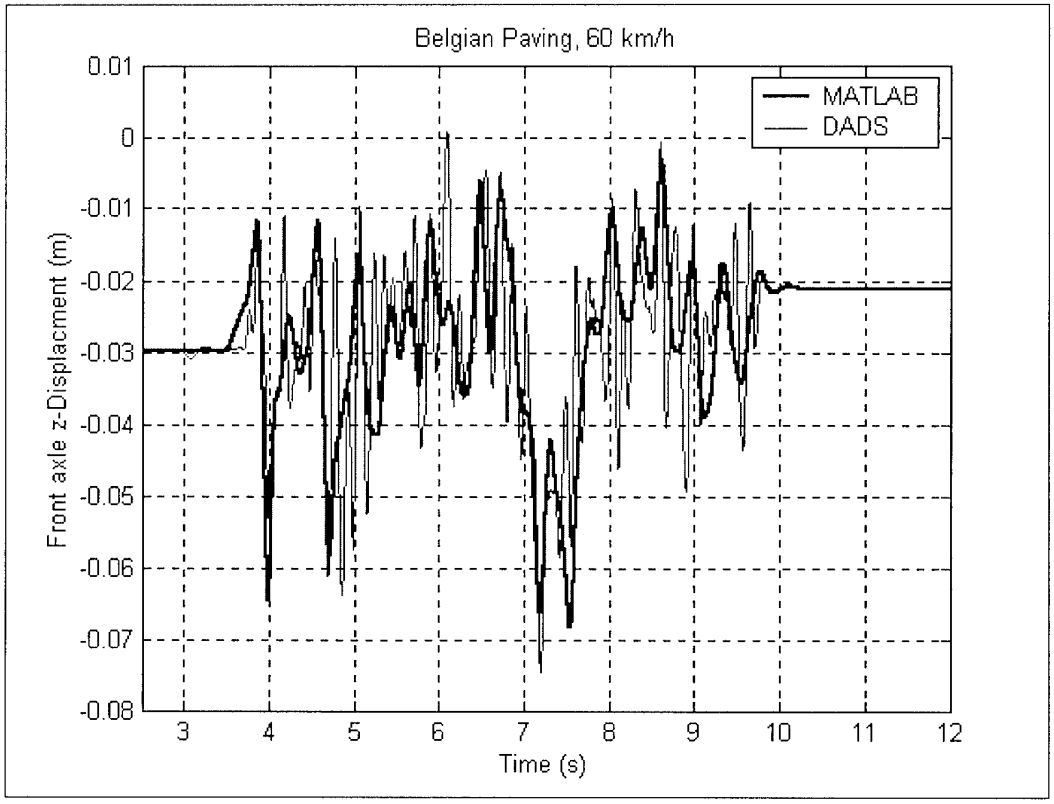

Figure 4 - Comparison of front axle vertical displacement predicted by MATLAB and DADS models for a Belgian paving road traversed at 60 km/h.

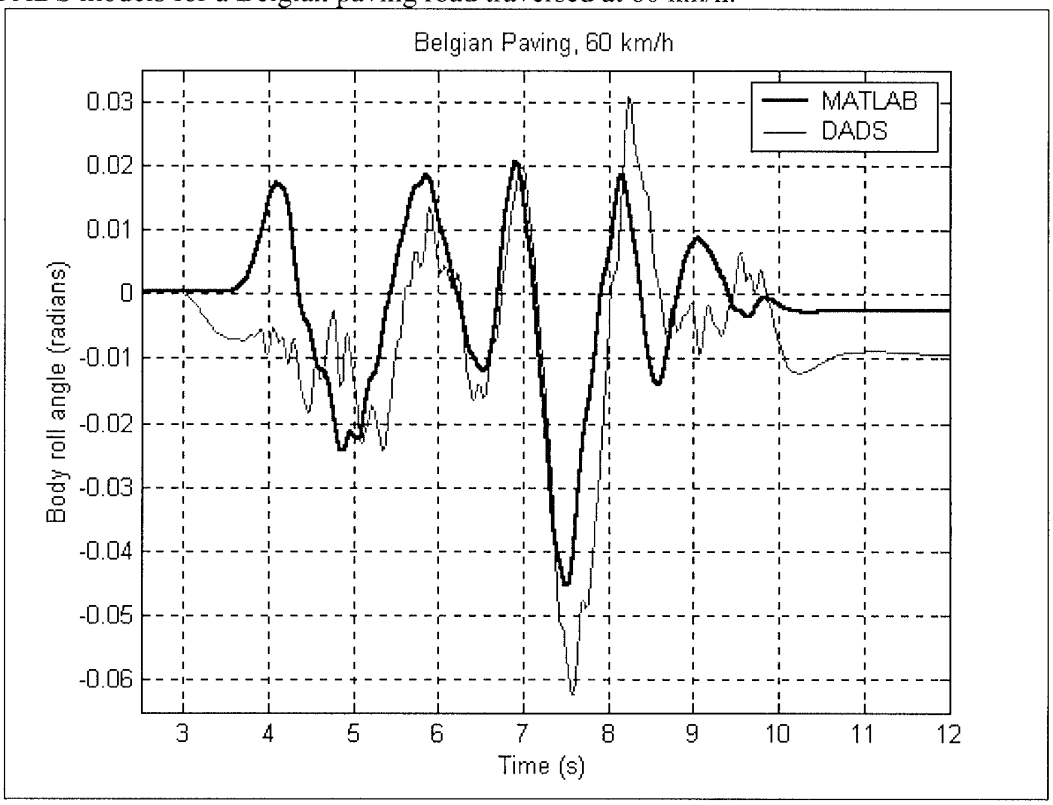

Figure 5 - Comparison of vehicle body roll angle predicted by MATLAB and DADS models for a Belgian paving road traversed at 60 km/h.

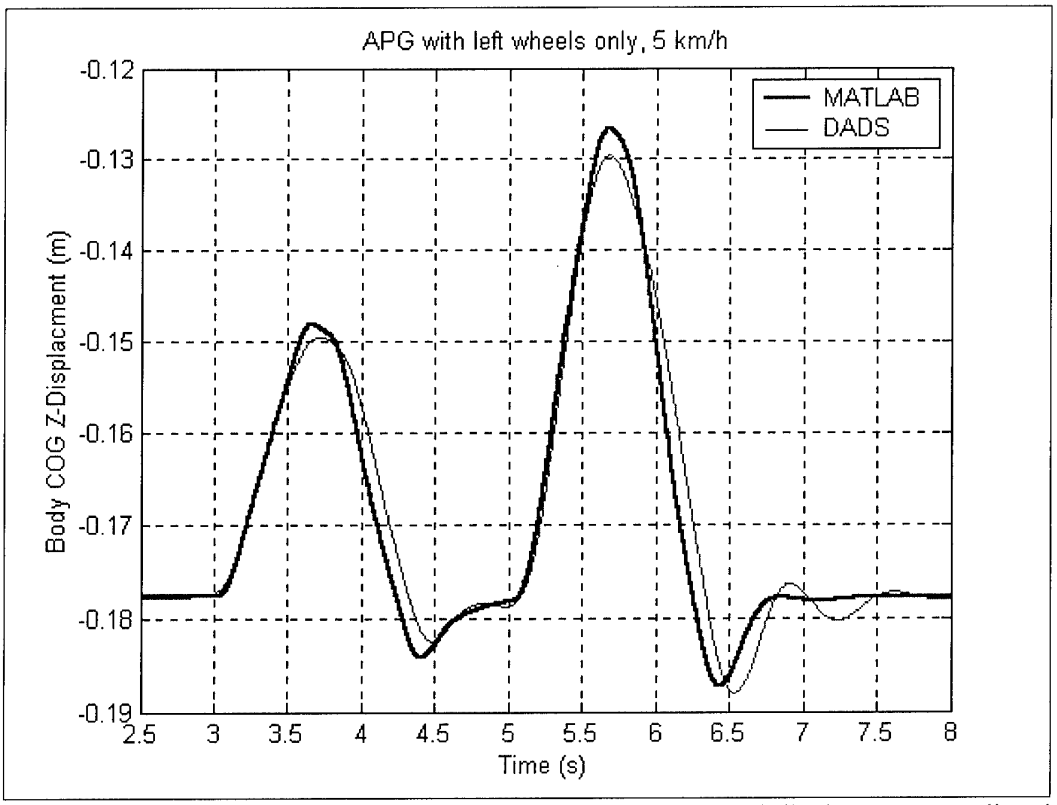

Figure 6 - Comparison of vehicle body center of gravity vertical displacement predicted by MATLAB and DADS models for an APG obstacle at 5 km/h with left wheels only.

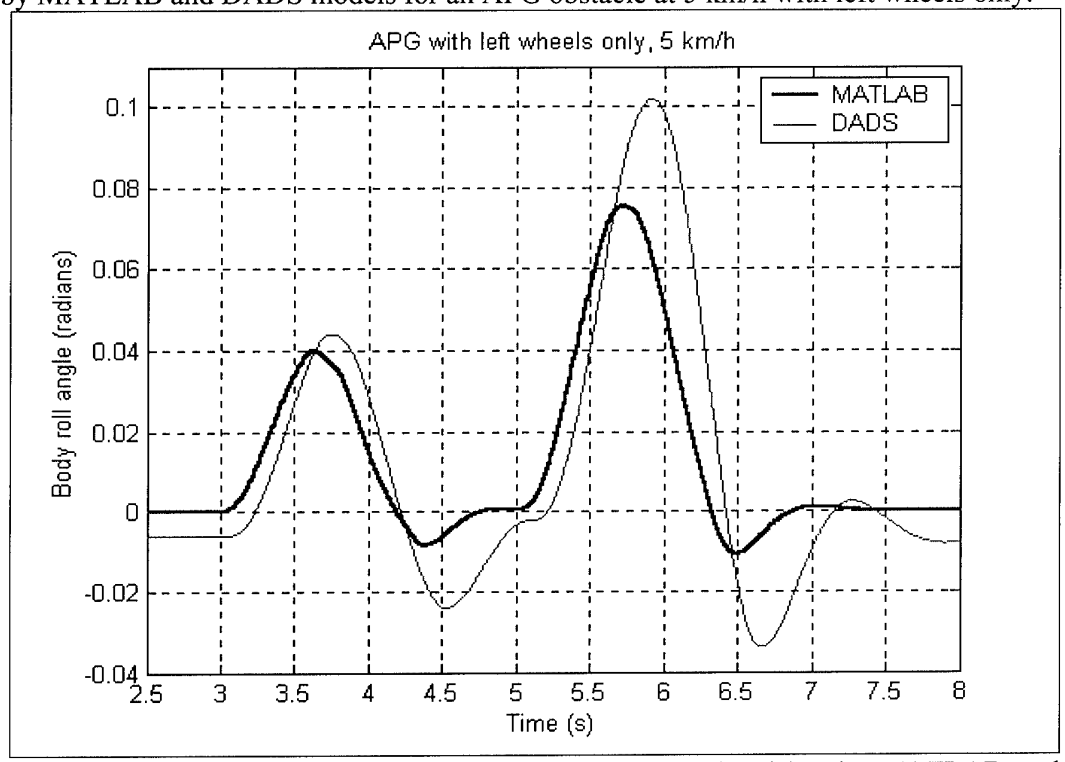

Figure 7 - Comparison of vehicle body roll angle predicted by the MATLAB and DADS models for an APG obstacle traversed at 5 km/h with the left wheels only.

3.2. Required suspension characteristics

The DADS model was used to predict ride comfort and handling of the vehicle with different combinations of spring and damper characteristics. Simulation results were used to determine first order indications of the "best" soft and hard characteristics for both the spring and damper.

The coil springs on the baseline suspension were replaced with hydro-pneumatic springs where the spring stiffness is determined by the gas volume in the static position. Static gas volumes were varied between 0.01 liter and 3.0 liter. This gives a range of spring stiffness from about 10 to 0.1 times that of the baseline coil spring stiffness. To simplify the damper characteristics, the baseline damper force was scaled with a constant factor that varied between 0.8 (i.e., softer than baseline) up to 3 (3 times higher than baseline). Simulations were performed for 7 damper characteristics and 10 spring characteristics within these ranges, giving a total of 70 simulation runs. Although this process was performed manually for the project, a study (not part of this project) is in progress to investigate the applicability of mathematical optimisation to the problem in an attempt to decrease the number of required simulation runs. Very positive preliminary results have been obtained as discussed in [27].

Ride comfort was simulated over a typical off-road terrain (Belgian paving block course) at a vehicle speed of 60 km/h. Ride comfort was evaluated using the vertical acceleration at the driver position (right front) as well as the left rear passenger position. The vertical acceleration was weighted using the British Standard BS 6841 weighting filter and calculating a weighted root mean square (RMS) value ([21], [22] and [23]). A three-dimensional plot of weighted RMS acceleration vs. spring static gas volume and damper scale factor is indicated in figure 8.

The lowest acceleration levels (best ride comfort) are obtained with low damping (damper scale factor of 0.8) and soft springs (static gas volume > 0.5 liters). Motion sickness values do however increase with very soft springs.

Handling was simulated by performing a severe double lane change manoeuvre [24] at a speed of 60 km/h for the same values of spring and damper characteristics used for ride comfort analysis. Maximum body roll angle was used as evaluation parameter for handling. Figure 9 indicates the results of the handling simulations. The smallest body roll angle is achieved with the stiffest spring (static gas volume of 0.01 liter) while the roll angle is insensitive to the damper scale factor as can be expected.

The "best" handling suspension is therefore at as high a spring stiffness as possible. The areas where there are gaps in the graph, are where the vehicle could not complete the lane change without rolling over.

It is concluded that for best ride comfort, a soft suspension is needed and for best handling a stiff suspension is needed. This is in line with general design rules and was the motivation for initializing this research project. The simulation results do however indicate that for the hard suspension setting, a static gas volume of 0.1 liter and damping scale factor of between 2 and 3 is suitable and for the soft suspension setting, a gas volume of greater than 0.5 liter and a damping scale factor of 0.8 will be suitable first order values for the design. The high damper characteristic used in the design of the

suspension system will therefor be between 2 and 3 times the baseline values, while the low damping should be less than 0.8 times the baseline value. More simulation will be performed at different speeds and over different terrain profiles at a later stage, but the current results are very useful for developing the suspension hardware.

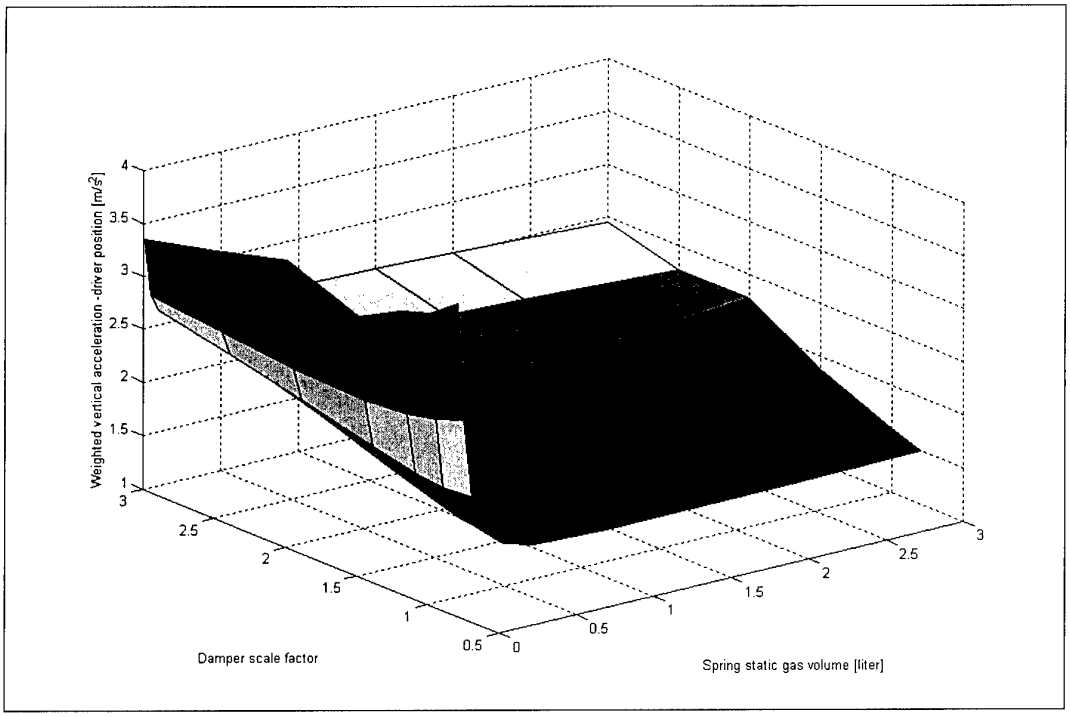

Figure 8 – Results of ride comfort analysis

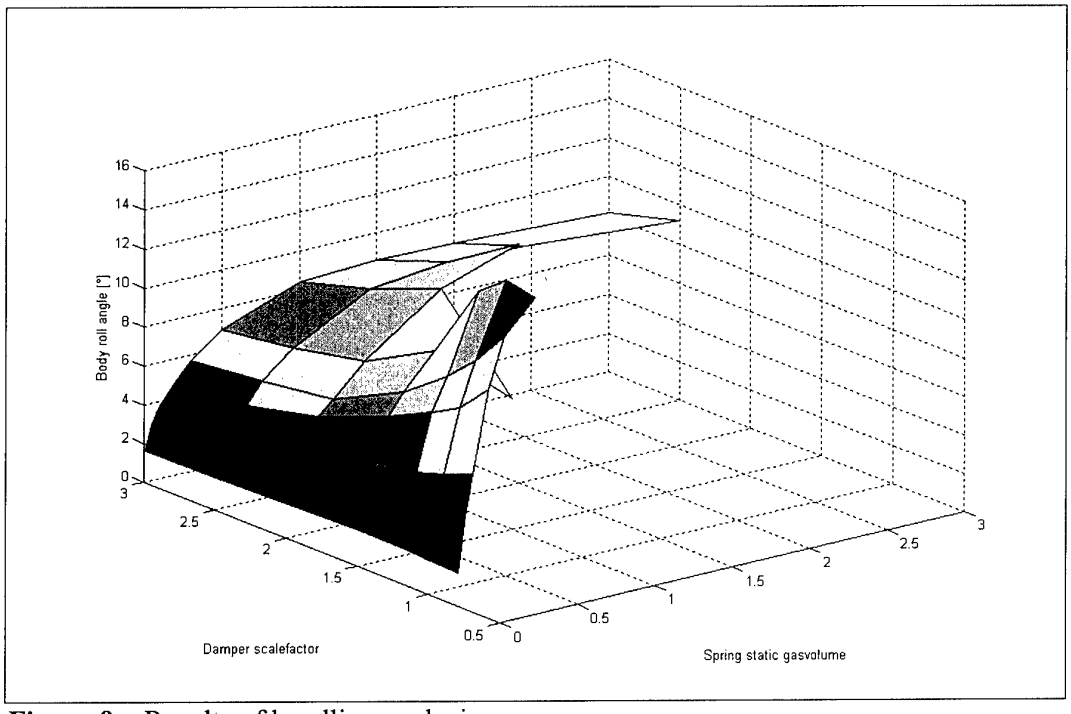

Figure 9 – Results of handling analysis

3.3. Development of suspension hardware

The high and low characteristics for both spring and damper are made possible by channelling hydraulic fluid with solenoid valves. The basic layout of the proposed suspension system is given in figure 10. The main strut is fixed between the vehicle body and the suspension system, replacing both the coil spring and telescopic damper. The main strut is connected to two piston accumulators via a valve block. All the control valves, hydraulic damper valves, control ports and channels are accommodated inside the valve block. On the prototype, provision is also made for four pressure transducers (P1 to P4) to measure pressures in the system.

The low spring rate is achieved by compressing a large volume of gas in the two separate piston accumulators. By sealing off the 0.4 liter accumulator with valve 3, a smaller gas volume is compressed and a higher spring rate is achieved. Spring rates can be individually tailored by changing the two gas volumes. For low damping, the hydraulic dampers (dampers 1 and 2) are short circuited by opening the bypass valves (valves 1 and 2). For high damping these valves are closed and the hydraulic fluid is forced through the dampers resulting in high damping force.

The main design specifications for the controllable suspension system can be summarized as follows:

i) Suspension travel of 300 mm (maximum compression to maximum rebound)
ii) Soft suspension static gas volume of 0.5 liter
iii) Hard suspension static gas volume of 0.1 liter
iv) Maximum system pressure at full bump of 20 MPa
v) Maximum flow of 230 liter/minute (2 m/s suspension velocity)
vi) Maximum suspension force of 40 kN (5x static force)
vii) Valve response time in the order of 50 milliseconds

To design the controllable suspension system for fitment to a Landrover Defender 110 sports utility vehicle, the space envelope available for the new suspension was determined by physical measurement on a vehicle. A controllable suspension system, with the required characteristics, was designed to fit in the space envelope.

The left front and left rear axle portions and wheel well details were measured for this purpose. Figures 11 and 12 indicate the left front wheel well with the original and new suspension systems respectively. Figures 13 and 14 compare the original and new suspension layout for the rear suspension system. The suspension system can be fitted in the available space although small changes to the body may be required. The new suspension system is narrower than the coil spring and this may result in more interior space in the vehicle.

Two views of the controllable suspension system are given in figures 15 and 16. Figure 15 shows the tire side and figure 16 indicates the side facing the chassis. The suspension system is mounted to the axle by means of a spherical thrust bearing and to the chassis rail via a rubber bush. The coil spring and damper mountings on the original suspension system was fixed directly to the vehicle chassis rails and not to the body panels (see figures 11 and 13). This necessitated the use of a side mounting configuration for the controllable suspension system so that the unit can be fixed directly to the chassis rail.

It is concluded that fitment of the controllable suspension system on the vehicle is feasible although minor modifications to body panels may be required.

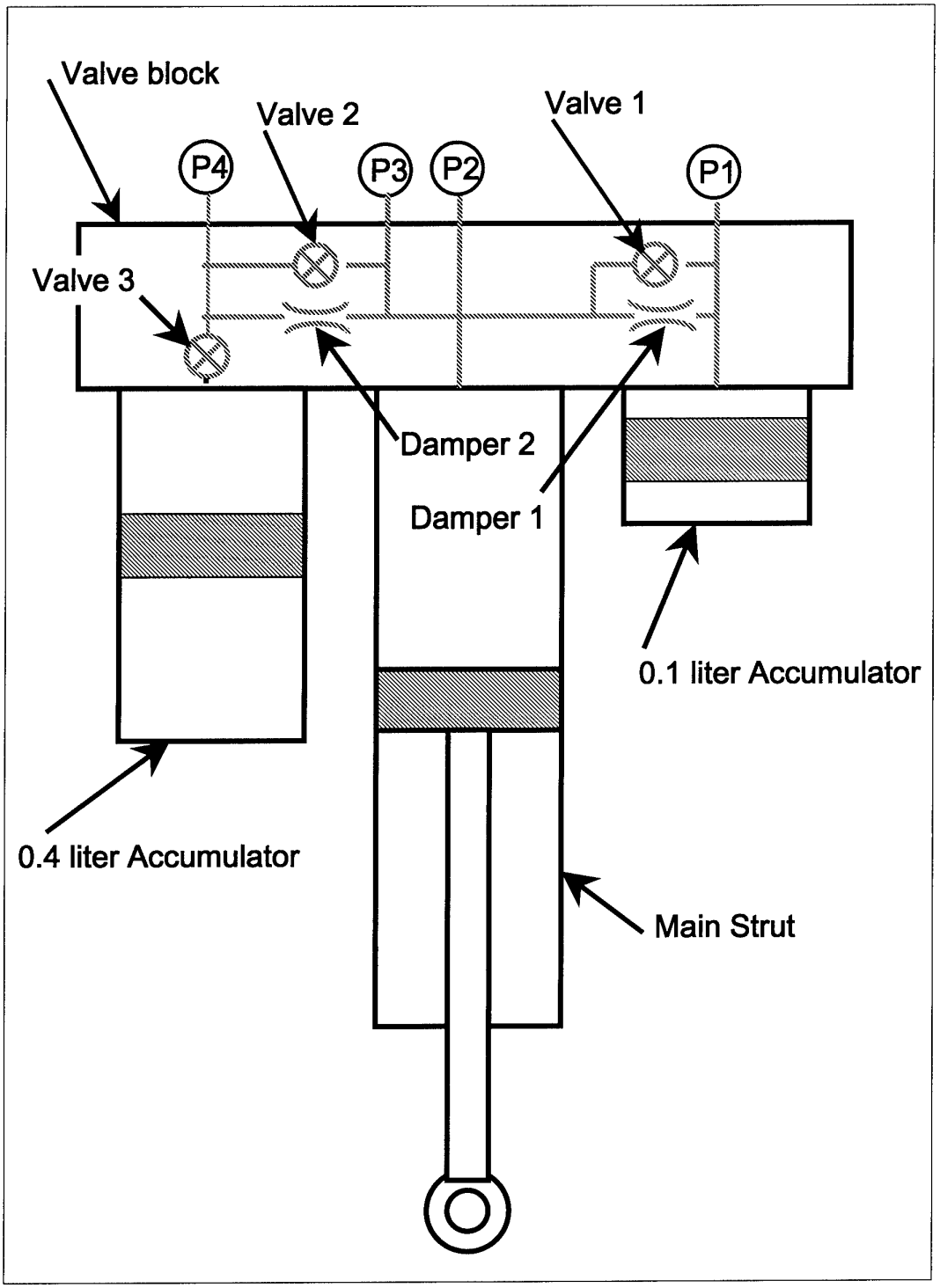

Figure 10 – Suspension schematic diagram

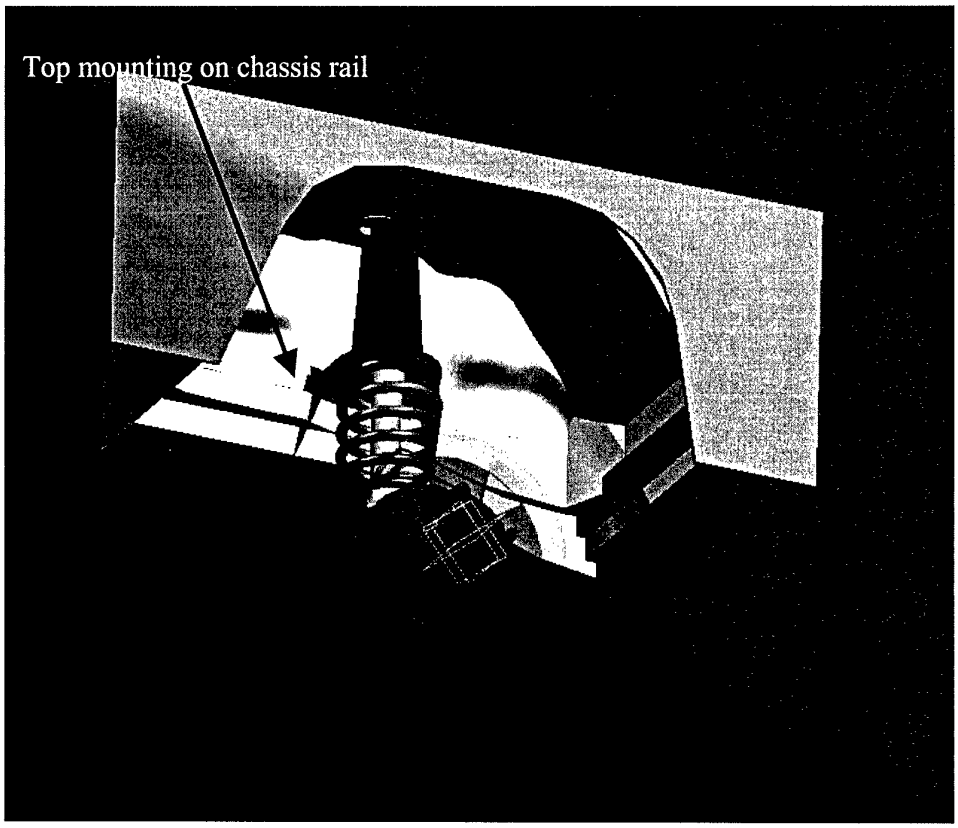

Figure 11 – Original front suspension layout

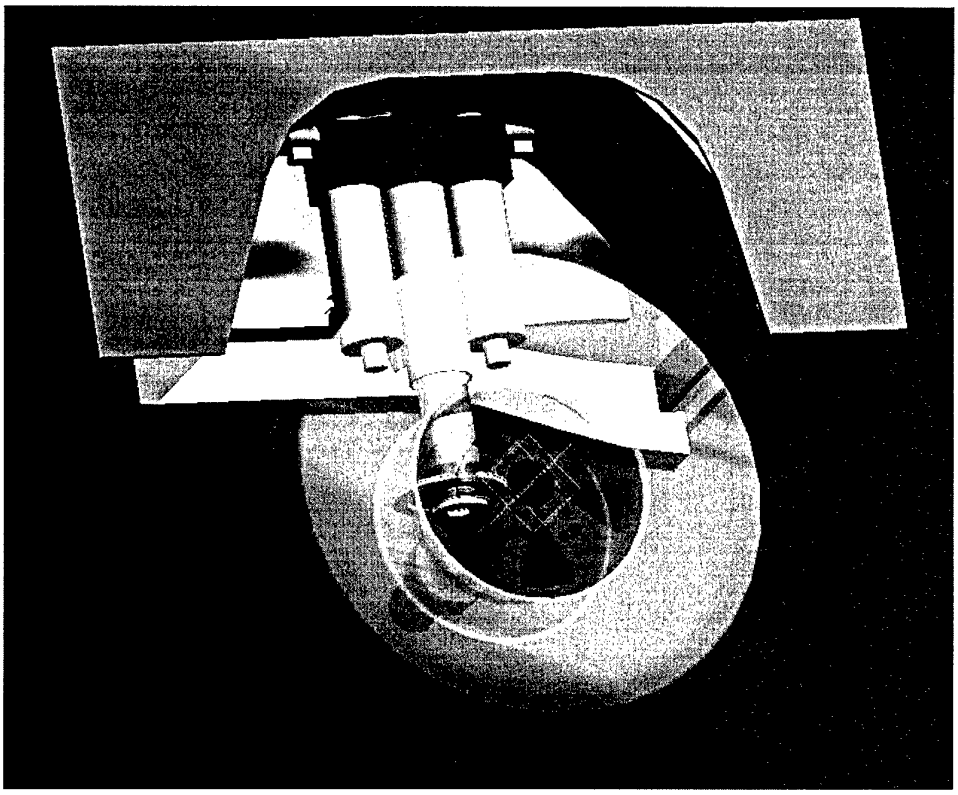

Figure 12 –Front suspension layout with controllable suspension system fitted

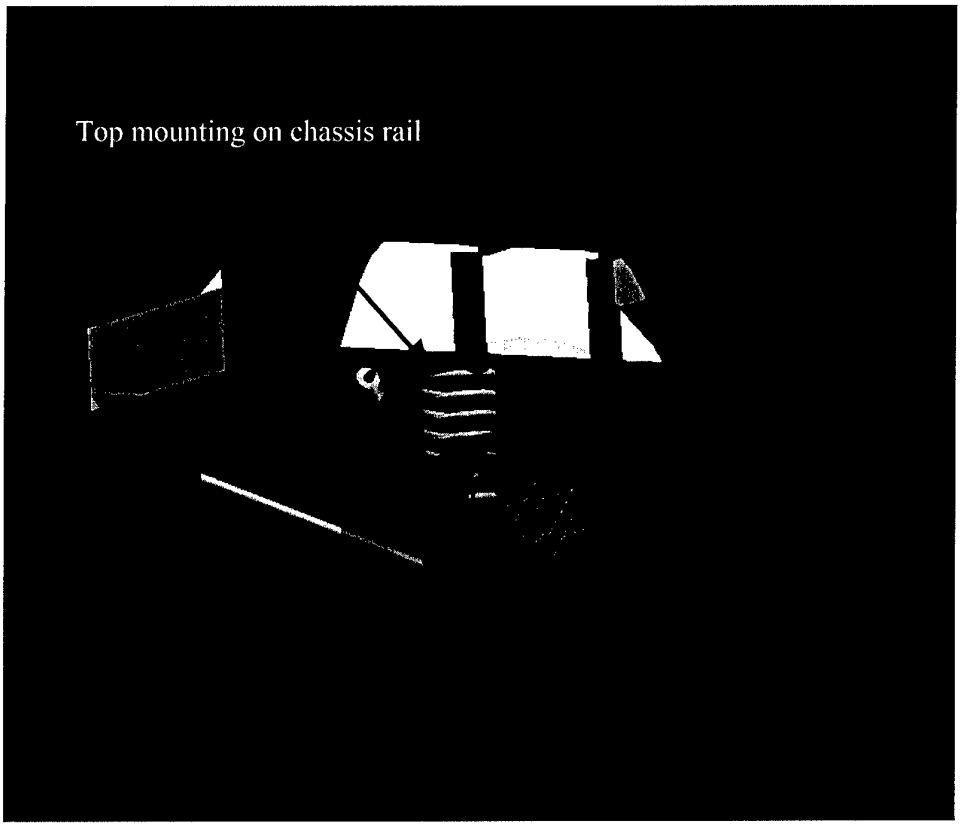

Figure 13 – Original rear suspension layout

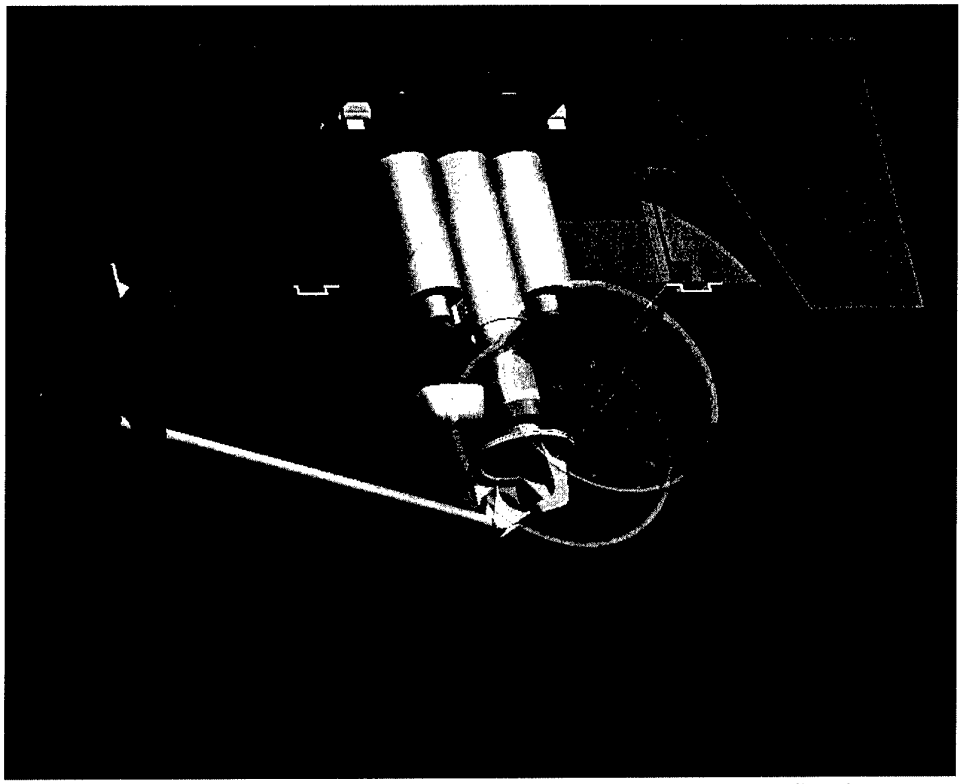

Figure 14 – Rear suspension layout with controllable suspension fitted

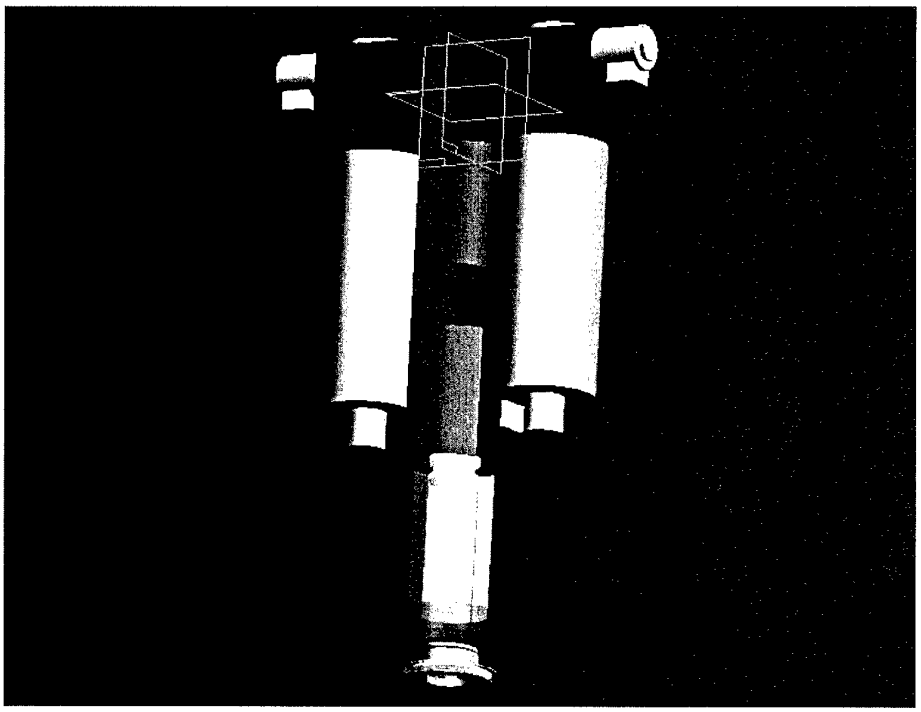

Figure 15 – Controllable suspension system – tire side

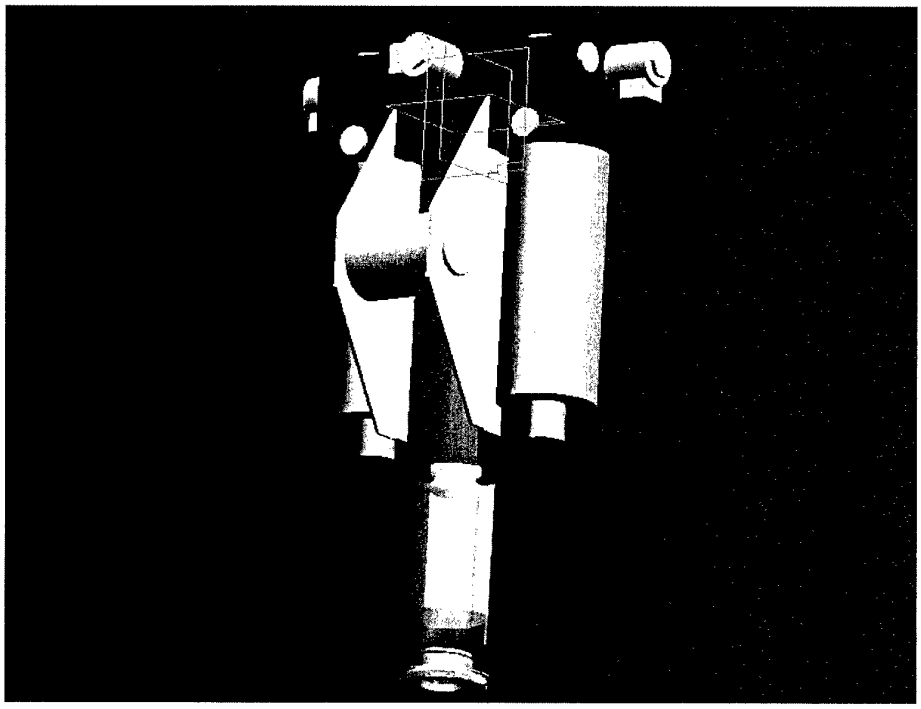

Figure 16 – Controllable suspension system – chassis side

3.4. Manufacture of prototype suspension unit

Detail design and design improvement of the controllable suspension unit have been performed. This included an investigation into different surface coatings, seals and sealing arrangements, as well as valves. The options considered for surface coatings at this stage is the normal hard chroming as well as a tungsten-carbide-cobalt coating

applied with a high velocity oxygen fuel (HVOF) process. The latter is very resistant to flaking and has extremely good wear resistance. For the prototype suspension unit, hard chroming was used and a comparison can be made between the two coatings during a later stage when improving the existing design.

Choice and availability of valves is a problem as a valve with a fast switching time is required. Standard valves available off-the-shelf can meet either the flow or the time response requirements, but not both. The design has therefore been modified to use two smaller, fast switching valves in parallel to handle the required flow and meet the switching time requirement. The valves used have previously been characterised for a different project at the University of Pretoria and information on response times is available [1].

The choice as far as sealing arrangements are concerned, is between sealing in the cylinder bore, or sealing on the piston rod. It is much easier to apply coatings to the rod, as well as to machine the rod to the required tolerances and surface finish. The rod sealing arrangement was therefore used in the prototype.

A set of manufacturing drawings have been compiled (see appendix B) and the system was manufactured by a company specializing in the manufacture of hydraulic equipment.

3.5. Testing and characterisation of suspension system

The prototype suspension was characterized on a test rig to obtain all the spring and damper characteristics as well as valve response times. A series of basic reliability tests was also performed to validate the choice of hydraulic seals and valves. The test rig consisted of a purpose designed test frame and a 100 kN SCHENCK hydropuls actuator (see figure 17). The prototype suspension unit was instrumented with four pressure transducers to determine dynamic system pressures. Actuator force and actuator displacement was also measured. The switching signal to the valves were recorded for determining the valve response times.

3.5.1. Spring characteristics

The isothermal spring characteristic was determined by slowly compressing the spring through it's operating range whilst recording force, displacement and pressure. Figure 18 indicates the spring force against spring displacement for the soft spring. Two curves are shown namely the force measured by the loadcell, and the force calculated from the pressure data. The measured force shows unacceptable levels of hysteresis, while the force calculated from the pressure measurement gives the expected characteristic.

During initial assembly of the unit, it was found that the main cylinder could be moved easily by hand, while the accumulator pistons had to be moved using compressed air. There was no way to move the accumulator pistons by hand. The hysteresis was therefore attributed to seal friction (stick-slip) in the accumulator seals. After considerable research, two new accumulator pistons were designed and manufactured using wear rings combined with a state-of-the-art accumulator seal with negligible stick slip. The original design used a fairly basic seal layout with a double o-ring and back-up ring system.

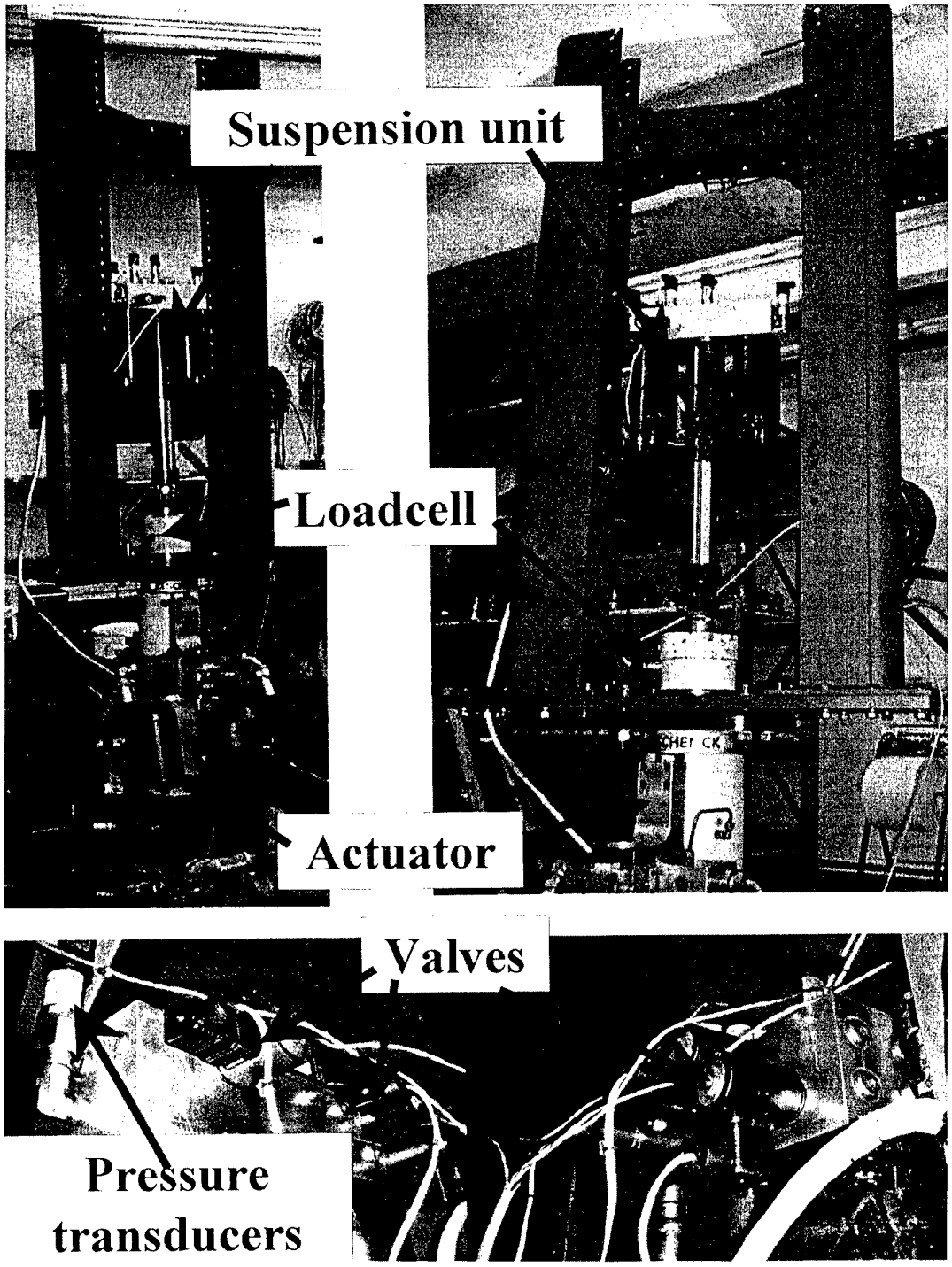

Figure 17 – Prototype suspension unit on test rig

After testing the more advanced sealing concept in the suspension system, it was found that the hysteresis had improved only marginally. Careful investigation traced the

problem to the bending moment applied to the main cylinder due to the offset chassis mounting arrangement (see figure 16 and Appendix B, figure B2). This results in a high side force between the main cylinder and the piston. This has not been proven yet, but seems to the be the only logical explanation. The mounting arrangement is in the process of being modified to eliminate the bending moment on the main strut. The rest of the data presented in this section was therefore calculated using the pressure measurements and not the actuator force.

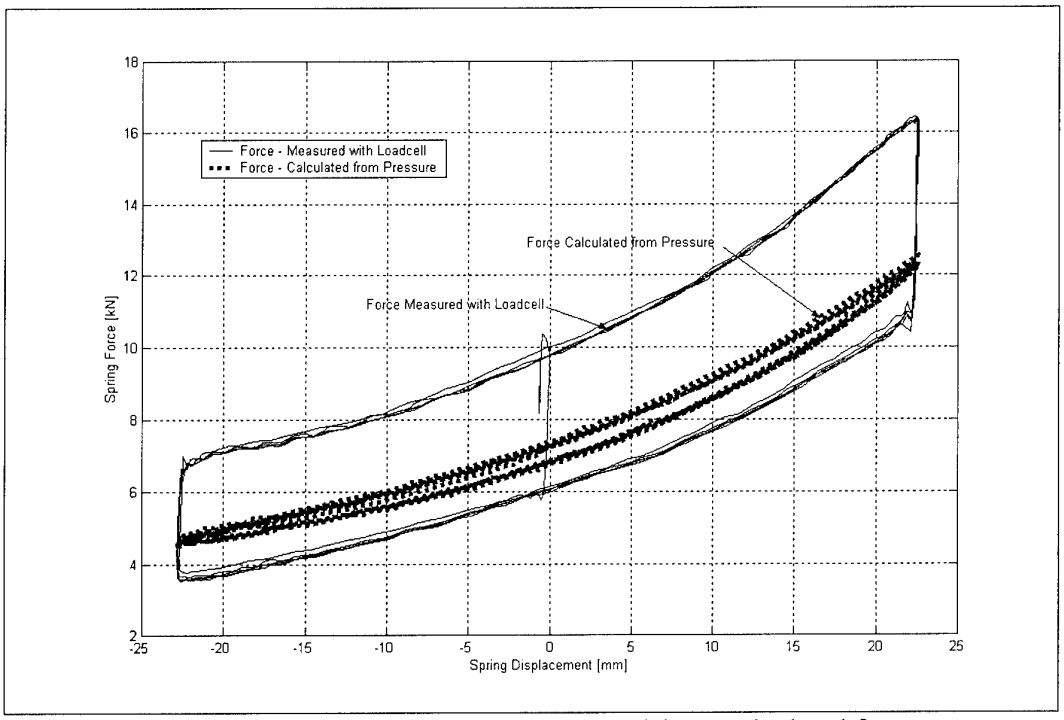

Figure 18 – Comparison between measured force and force calculated from pressure

The two spring characteristics were determined by displacing the actuator slowly with a sawtooth input displacement. Figure 19 gives the soft spring characteristic measured for one complete compression and rebound cycle lasting 300 seconds. The measured value is compared to the predicted isothermal spring characteristic and excellent correlation is observed. The small hysteresis loop in the measured characteristic can be attributed to heat transfer between the gas and the surroundings. This effect is well documented in [11].

Figure 20 gives the stiff spring characteristic measured for one complete compression and rebound cycle. The displacement cycle starts in the static position, compresses the spring to 40 mm, extends the spring to –100 mm, compresses the spring again to +40 mm and then returns to the static position. This cycle lasts 300 seconds. The measured value is again compared to the predicted isothermal spring characteristic, but in this case there is a significant discrepancy between measured and predicted results. The hysteresis loop in the measured characteristic can again be attributed to heat transfer between the gas and the surroundings. Further investigation indicated that the discrepancy in the stiff spring characteristic can be attributed to the compressibility of the oil (usually deemed negligible). Figure 21 indicates two straight lines corresponding to a bulk modulus of 1.5×10^9 N/m^2, and a force displacement characteristic measured with the suspension unit full of oil, but with no gas in the accumulators (i.e. with both accumulators against their

end stops). The compressibility is therefore significant for the stiff spring characteristics and needs to be taken into account during spring calculations. The figure also indicates the very good correlation achieved when the spring characteristic is corrected using the bulk modulus. Figure 22 indicates measured and calculated characteristics for both the soft and stiff springs.

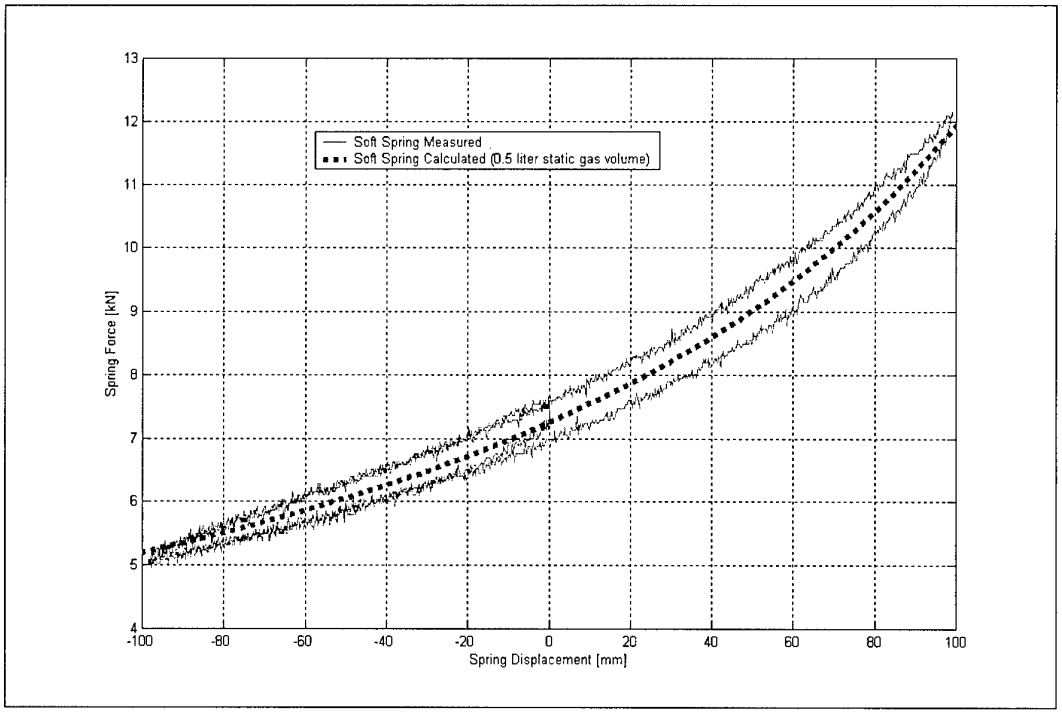

Figure 19 – Soft spring characteristic

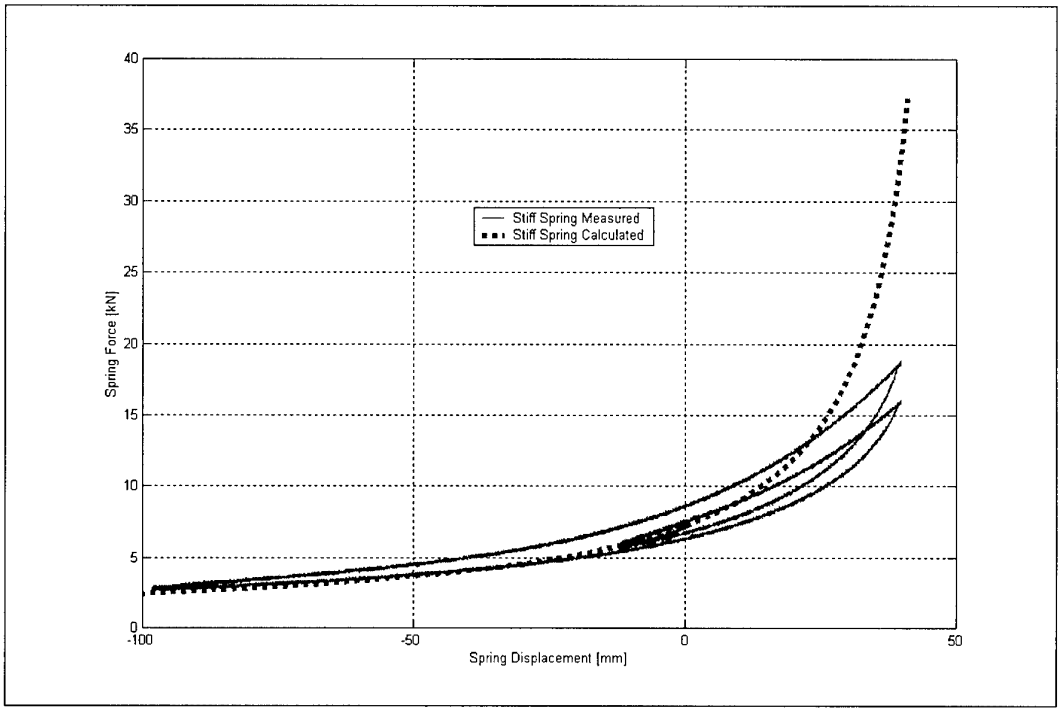

Figure 20 – Stiff spring characteristic

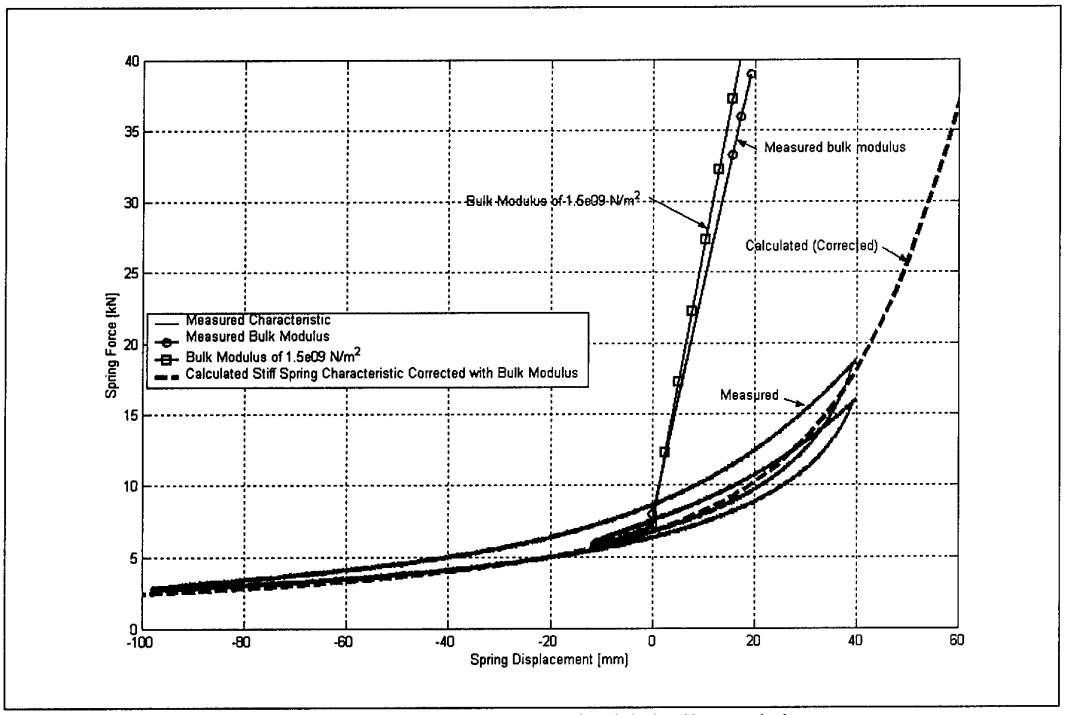

Figure 21 – Stiff spring characteristic, corrected with bulk modulus

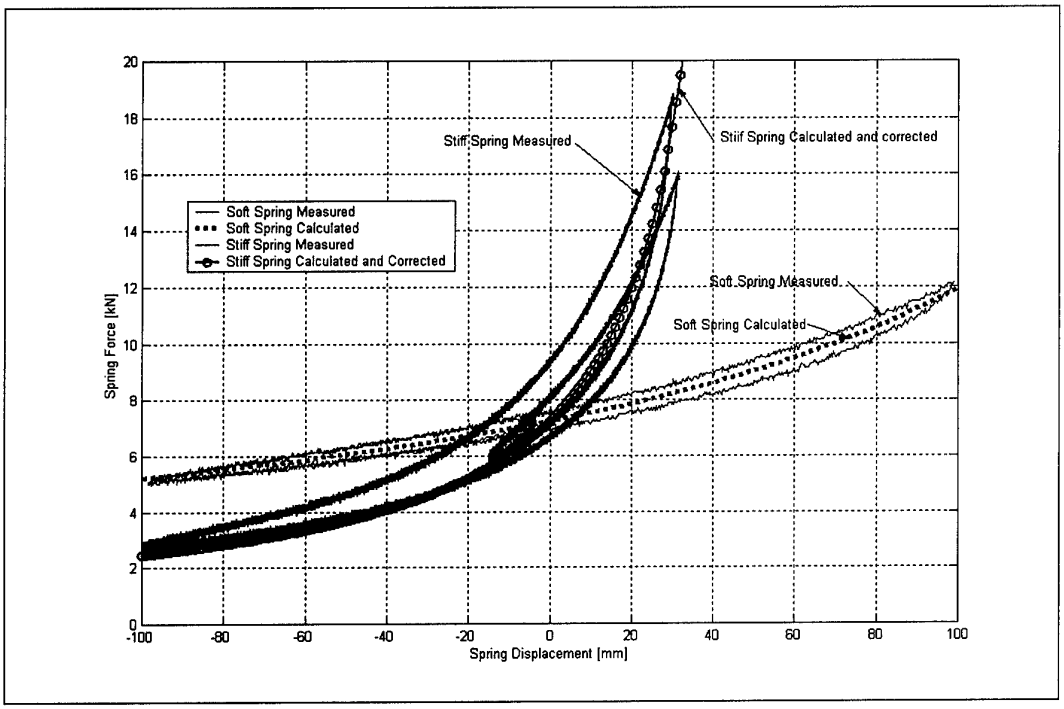

Figure 22 – Soft and stiff spring characteristics

3.5.2. Damping characteristics

The damper packs in the strut were taken from standard Landrover rear dampers.

Figure 23 indicates the damping characteristics measured on the suspension unit. Damping characteristics were determined by exciting the strut with a sinusoidal input displacement with a displacement of 25 mm (total stroke of 50 mm). The frequency of the sine wave was varied to give different velocities. Force values were calculated from the pressure readings.

Three different characteristics were measured on the strut namely the soft damping characteristic (both dampers bypassed), high damping characteristic (no bypass) with soft spring and high damping characteristic (no bypass) with stiff spring. For reference, the required (baseline Landrover) characteristic, as measured on a Landrover damper, is also indicated on the graph. The strut damping characteristics were expected to be higher than the baseline dampers due to the increased piston area as well as increased flow. This was found not to be the case and the difference can be attributed to a manufacturing error by the subcontractor. This manufacturing error means that the damper packs don't properly seal inside the valve block cavities, and fluid is leaking past the damper. This problem is in the process of being rectified. The results do however indicate that there are three discrete damping levels associated with the strut, i.e. the dampers can be switched between high and low damping characteristics. The damping level will be increased to the required levels once the sealing problems have been rectified.

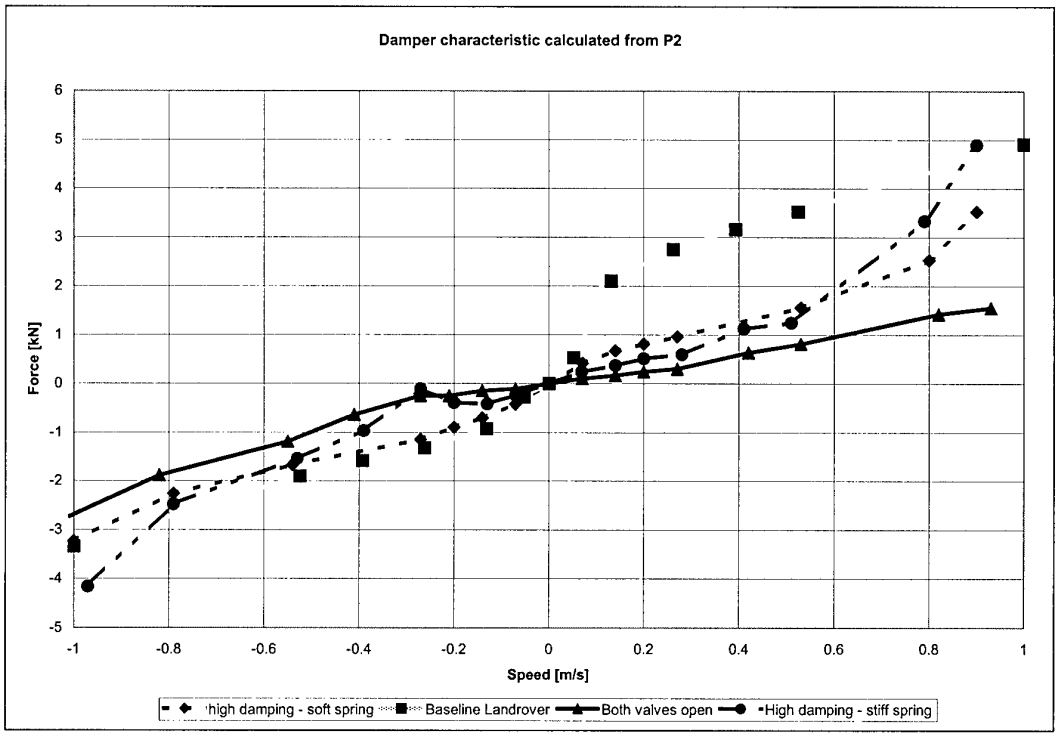

Figure 23 – Damper characteristics

3.5.3. Valve response times

A typical trend of pressure drop over the valve vs. time is shown in figure 24. The solenoid switching signal is indicated on the same graph. To obtain the valve response time, the initial pressure difference (before switching) and the final pressure difference (after the transient response has died away) is determined. Two values (represented by horizontal lines) are then calculated representing a 5% change and a 95% change in pressure difference respectively. This is done to define the switching points more precisely as the exact moment where the change occurs is very difficult to determine. The time from the solenoid switching signal to the 5% change point is defined as the initial delay. This is the time required for the solenoid to build up enough force so that the valve plunger starts moving. The time between the 5% and 95% point is defined as the response time of the valve and represents the time required from the initial plunger movement until the valve is fully open. The total valve response time is the sum of the initial delay and the response time as indicated in figure 25.

The valve response time was measured by closing valve 3, compressing the strut until a required pressure difference was obtained, and then opening the valve. This resulted in flow through the valve until the pressure in the system stabilized.

The valve response time is to some extend dependant on the system ([1]). Values are also dependent on the pressure difference across the valve as can be seen in the figure. The valve response time varies from 40 to 90 milliseconds over the pressure range of interest and this is very acceptable for the current application.

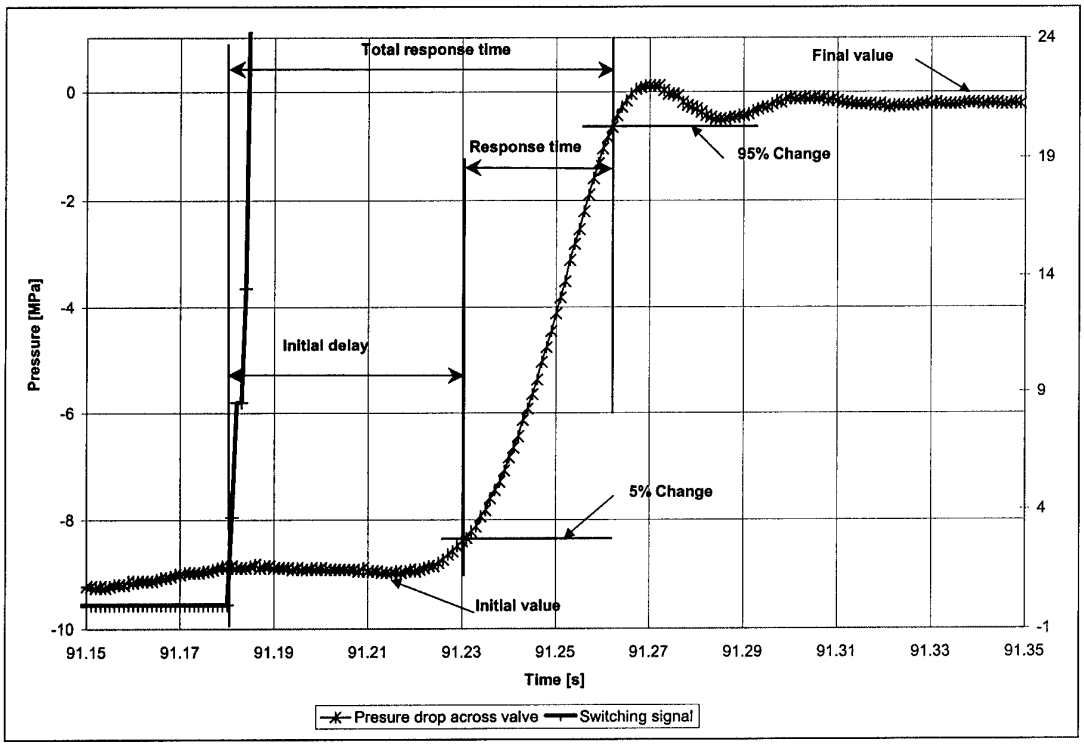

Figure 24 - Explanation of valve response time definitions

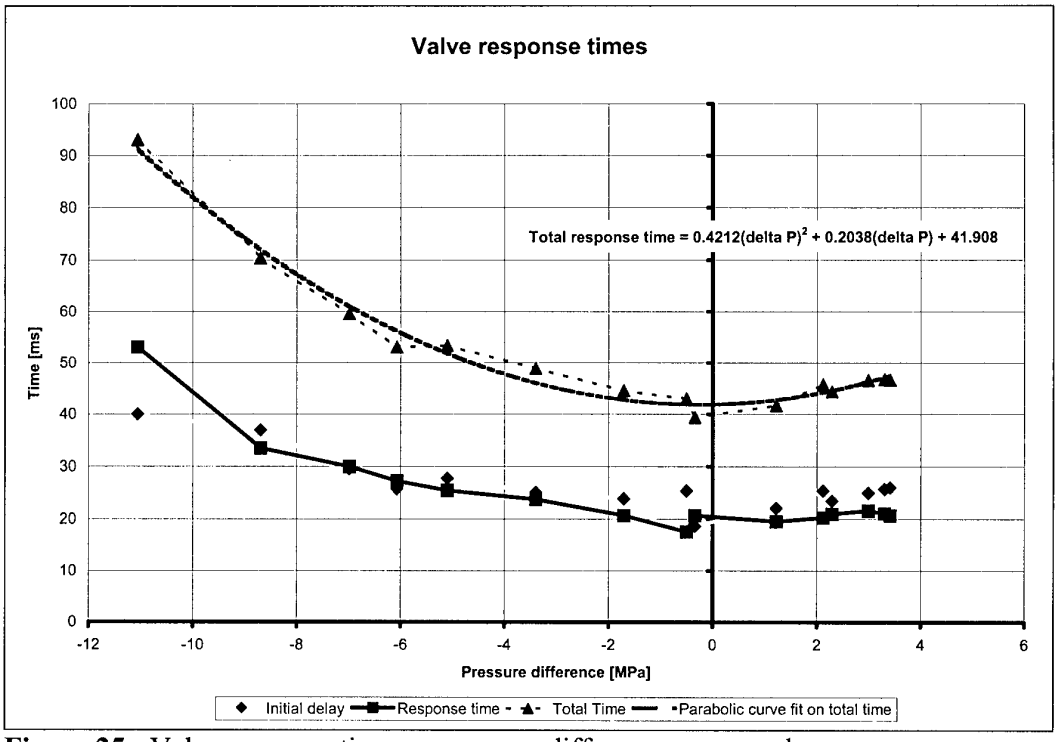

Figure 25 - Valve response time vs. pressure difference across valve

3.6. Mathematical models of suspension unit

A mathematical model that can predict the spring and damper characteristics (including valve response times) of the semi-active suspension unit was developed in SIMULINK. The block diagrams of this model and its subsystems are shown in figures 26 to 30.

The model accepts five input signals: the displacement of the suspension unit from its reference position (compression positive), the compression speed of the unit and the three switch signals (for valves 1, 2 and 3 in figure 10) that can each take only the values of 0 and 1, 0 indicating a closed valve condition and 1 an open vale condition. For these inputs the model calculates the spring-damper force of the unit, positive for a compressive force. The purpose of the model is to serve as a sub-system in a larger model for simulating the vehicle dynamic response. The vehicle model incorporating four of these the suspension units (one for each wheel station) as well as a control module for controlling the four units will be developed in the next phase of the project. The vehicle dynamics model will be developed in the ADAMS environment and will be coupled to four SIMULINK models of the suspension unit, feeding these the respective suspension unit displacement and speed signals and receiving from these the suspension forces for consideration in the vehicle dynamics simulation. The control module will generate the 4 x 3 valve switch signals.

In the suspension unit SIMULINK model the spring and damper forces are calculated employing a table look-up procedure with linear interpolation. The look-up tables were generated from calculated data based on isothermal compression of the spring. This part of the model may be upgraded in future to take heat transfer effects (as modeled in [3]) into account if deemed necessary. When any one of the valves switches from one position to the other, the look up procedure switches to a different table. This happens

instantaneously, even though the switching point is delayed with respect to the switching point in the switch signal, to account for the valve response time. The valve response time is dependent on the pressure drop over the valve. This dependency was measured in the laboratory and a parabolic function was curve fitted to the measured data (see figure 25). The parabolic function is built into the SIMULINK model as part of the sub-system "Pressure dependent valve switching", the block diagram of which is shown in figure 27 (the function block accepting the "Delta P" input in input 2). The damper force divided by the cylinder area is used as an approximation of the pressure drop over the valve, in the case of the two damper valves, while the spring force is used in a similar manner with respect to the spring valve. In actual fact the switching is accompanied not only by a delay but also a smooth transition from one curve to the other, rather than a step change. This smooth transition is not modeled at this time. It is planned, however, to include this aspect in a second-generation model of the suspension unit, to be developed during the next phase of the project.

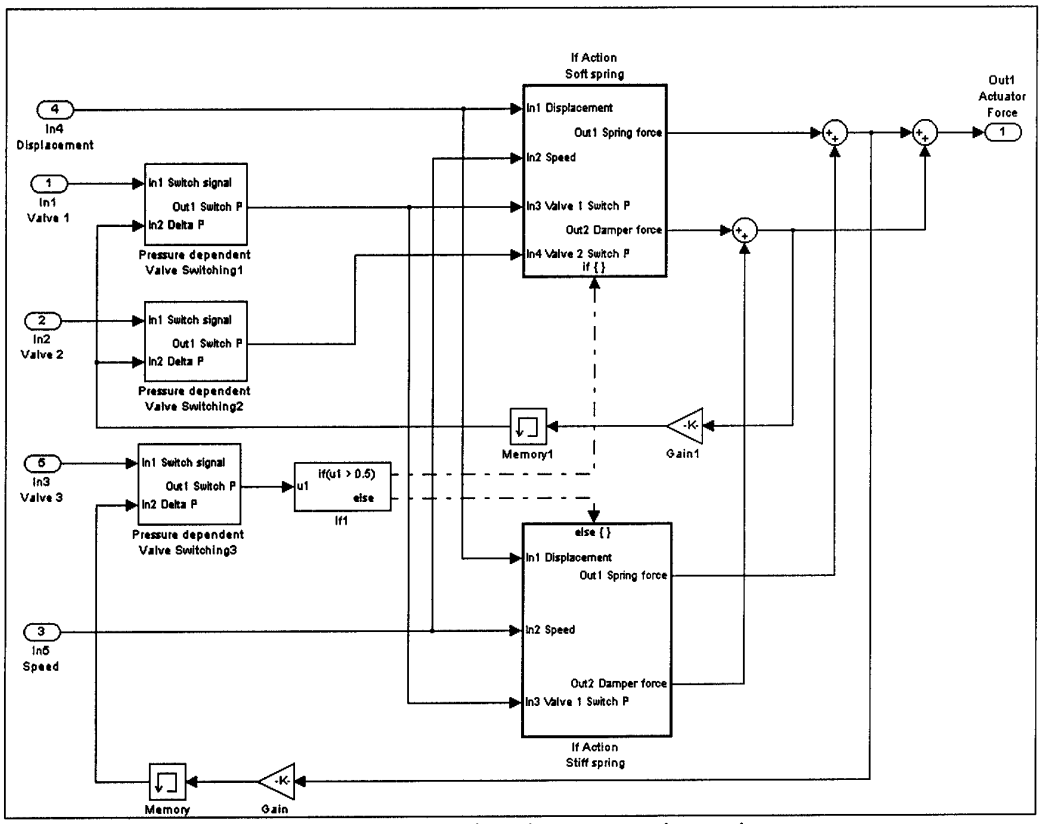

Figure 26 - Simulink model of the semi-active suspension unit.

If the spring valve (valve number 3) is switched to have a soft spring, the model executes the sub-system "If action soft spring", the block diagram of which is shown in figure 28. This sub-system takes the spring displacement as input and interpolates on the soft spring curve to give the spring force as output. It furthermore takes as input the two damper valve pressure switch signals to determine on which of the high or low damping curves the interpolation should be done. This interpolation is carried out by either of the sub-systems "If action low damping" or "If action high damping". The block diagram of the former is shown in figure 29, and is typical of all the damper interpolation sub-systems used in the rest of the model.

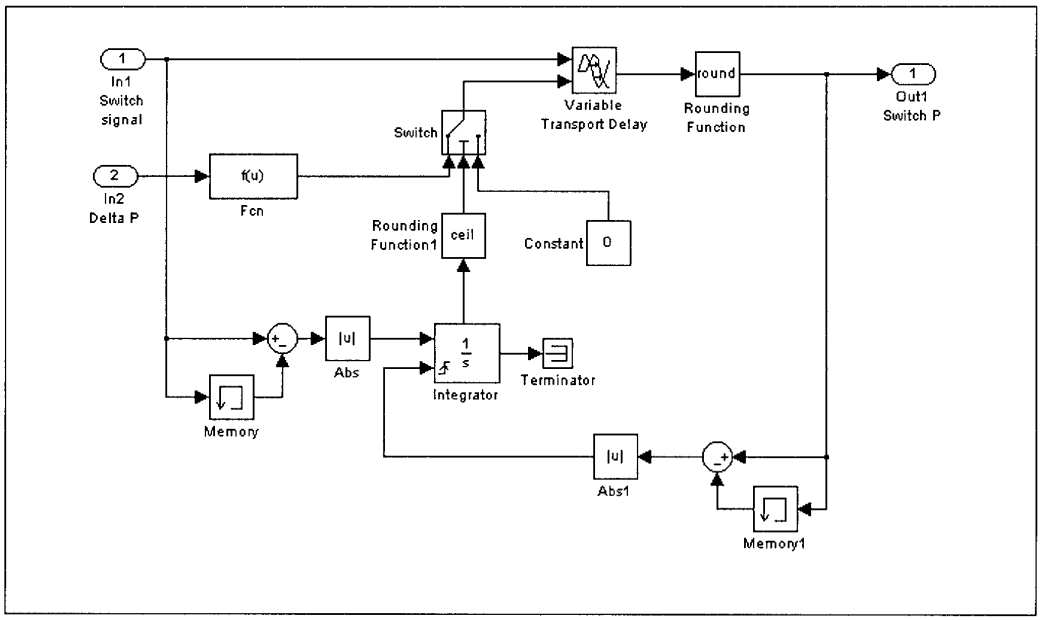

Figure 27 - Block diagram of the sub-systems (three of) "Pressure dependent valve switching", shown in figure 26.

If, on the other hand, the spring valve is switched to have a stiff spring, the model executes the sub-system "If action stiff spring", the block diagram of which is shown in figure 30. In this case the damper valve number 2 is inactive, so that this sub-system operates quite similar to the soft spring sub-system described above, only with one damper valve input.

The model at this time provides for switching between springs only when the suspension unit is at its reference displacement condition. It is planned that the next generation model to be developed in the next phase of the project will remove this limitation.

The way the suspension model works is illustrated to some extent by the graphs from a simulation run shown in figures 31 to 33. The input to the model is shown as the displacement and speed graphs in figure 31 and the three valve switch signals shown in figure 32. This figure also shows the respective switch signals in pressure and when this is compared to the corresponding valve switch signals the effect of the pressure dependent valve response time (delay) is evident. When the damper valves (valves 1 and 2) switch from 0 to 1 it means that the damper characteristic will switch from high to low damping. When the spring valve (valve 3) switches from 0 to 1 it means that the spring stiffness characteristic will switch from stiff to a soft.

Figure 33 shows the resulting suspension unit output force as calculated by the model.

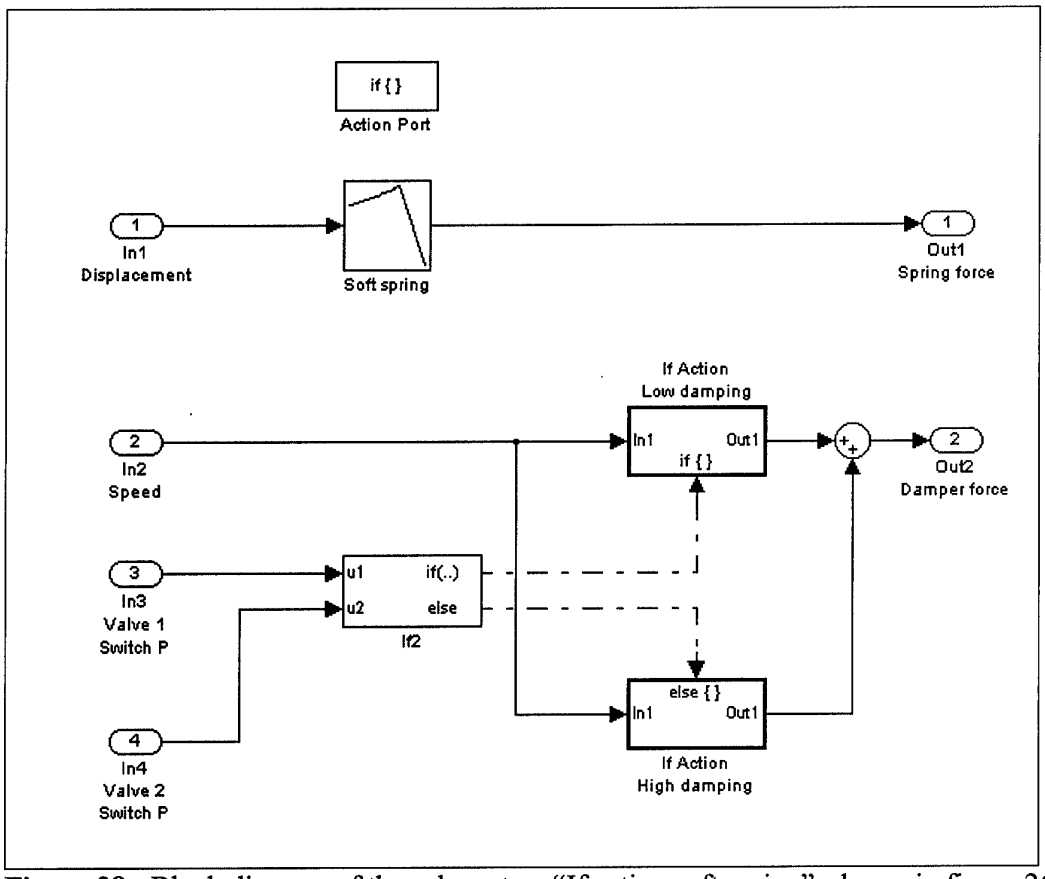

Figure 28 - Block diagram of the sub-system "If action soft spring", shown in figure 26.

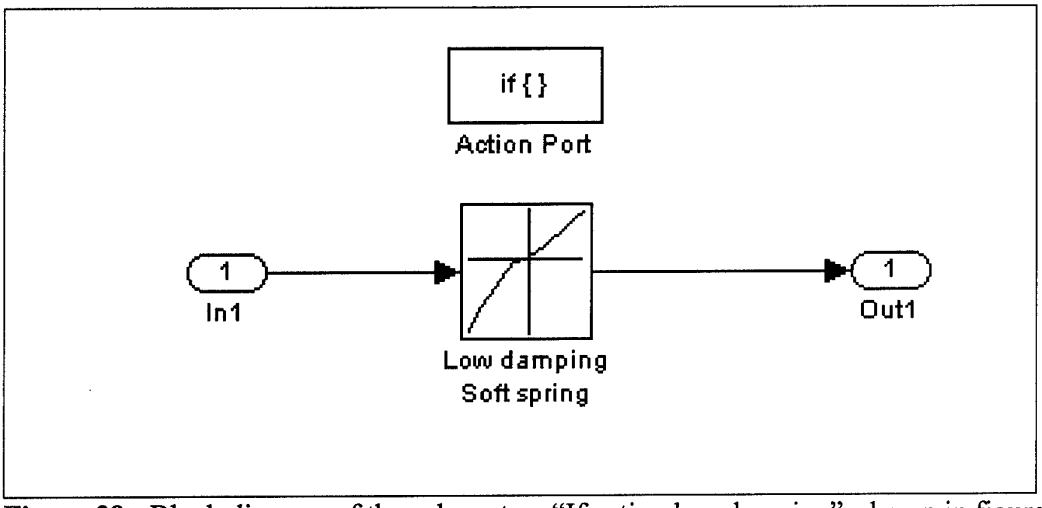

Figure 29 - Block diagram of the sub-system "If action low damping", shown in figure 28.

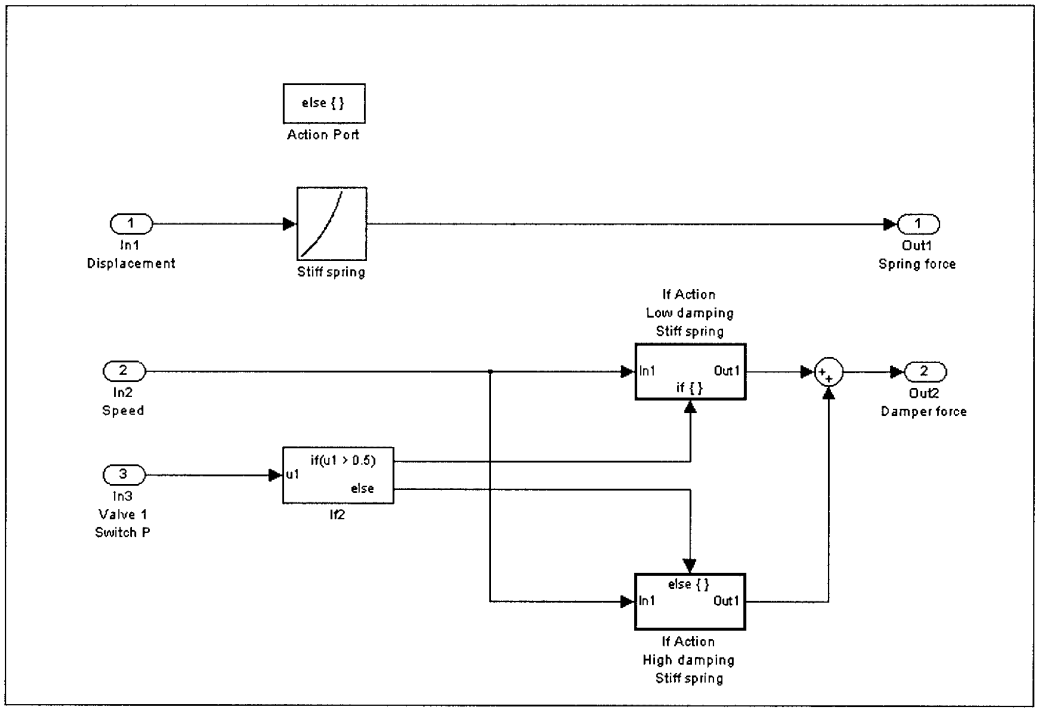

Figure 30 - Block diagram of the sub-system "If action stiff spring", shown in figure 26.

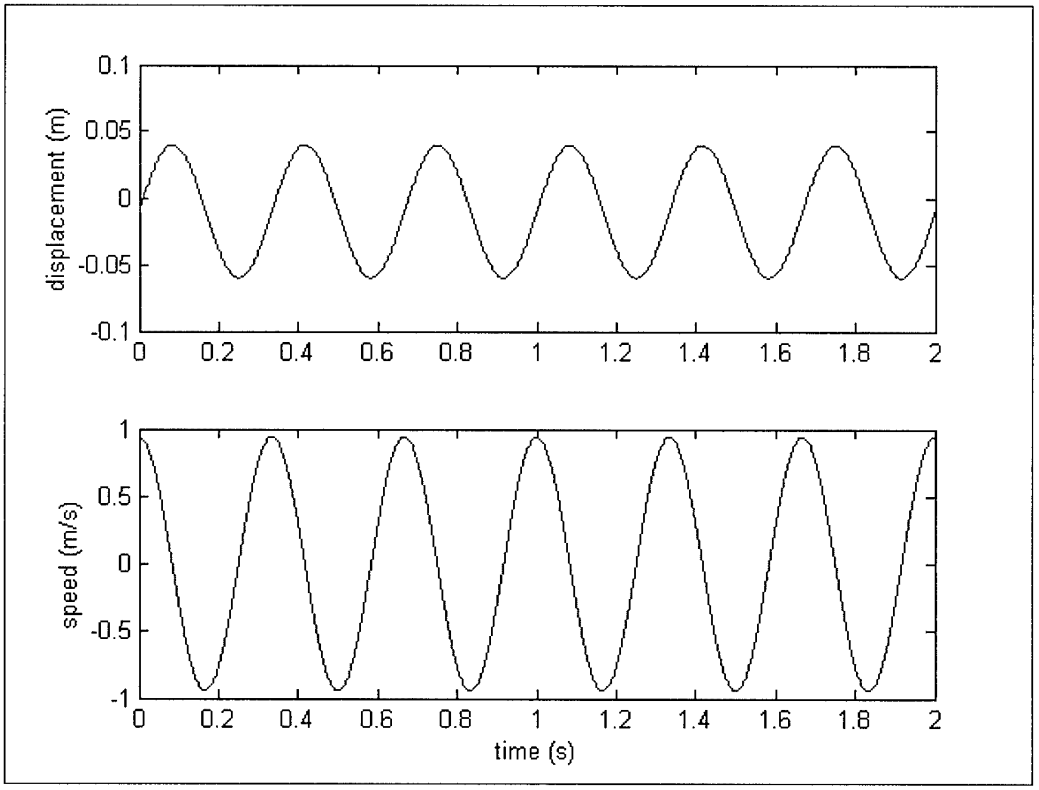

Figure 31 - Illustrative displacement and speed inputs to the suspension unit model.

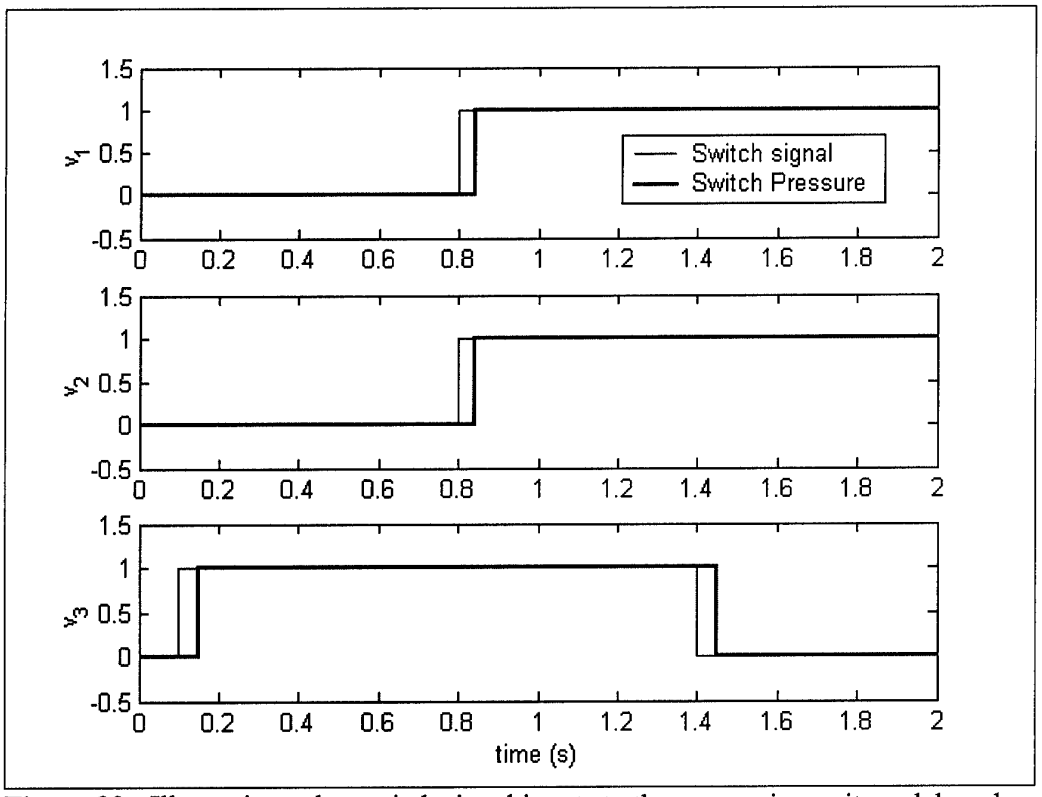

Figure 32 - Illustrative valve switch signal inputs to the suspension unit model, and delayed pressure switch signals as calculated by the model.

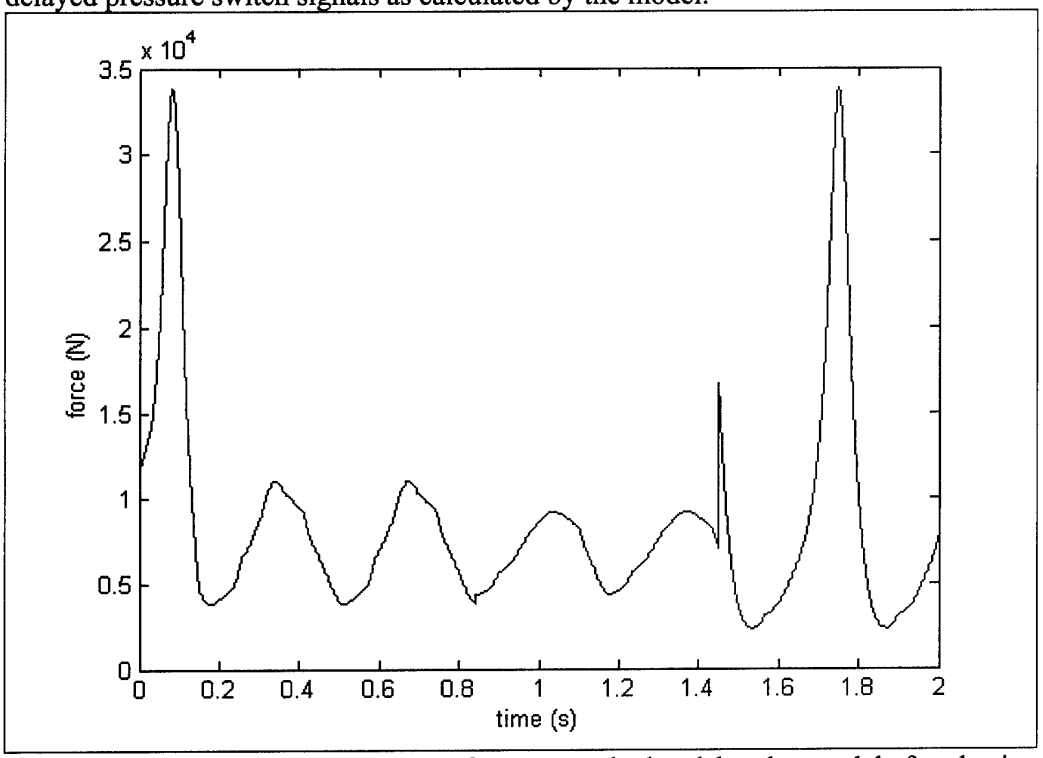

Figure 33 - Suspension unit output force, as calculated by the model, for the input signals of figures 31 and 32. Note that the switching between stiff and soft spring characteristics was not executed at the suspension unit reference position, as it should actually be done at this time.

A comparison was made between the spring force calculated by the SIMULINK model and measured in the laboratory on the first prototype suspension unit for a certain prescribed compression time history. During this time history the spring valve initially is closed so that the stiff spring characteristic is selected. Towards the end of the time history the valve is switched to open, to select the soft spring characteristic. The SIMULINK model was switched using the same signal as used in the experiment. The results are shown in figure 34. The model result is seen to compare very favorably with the measurement. The small differences are attributed to heat transfer effects as well as friction in the seals.

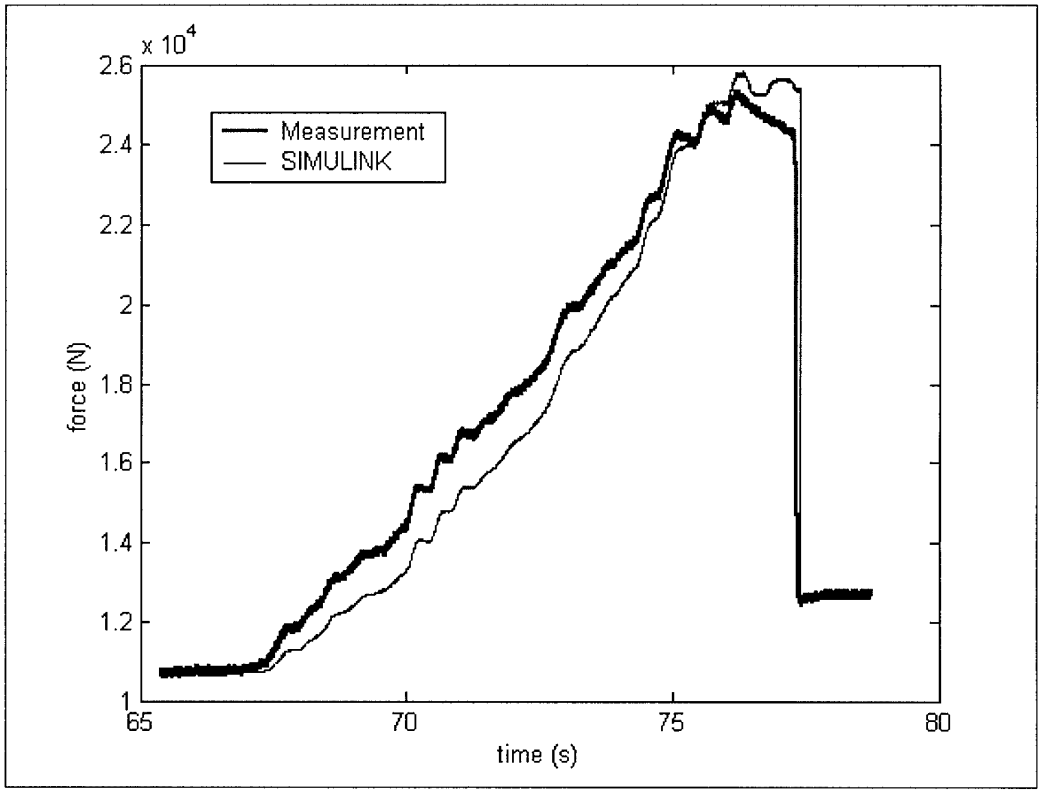

Figure 34 - Comparison between measured and SIMULINK predicted spring force time histories.

4. Conclusions

Mathematical models of the vehicle have been successfully developed and used to obtain the required spring and damper characteristics.

The feasibility of a two-stage semi-active damper, combined with a two-stage semi-active hydropneumatic spring was demonstrated. The proposed system was designed, manufactured and tested. Although certain problems exist, possible causes for the problems have been indentified. The solutions to these problems will be seeked and implemented during the next phase of the project.

Spring characteristics can be predicted with good accuracy, but the bulk modulus of the fluid needs to be taken into account at higher pressures.

Two discrete damping characteristics have been demonstrated, although the values for the high damping characteristic is too low for the current application. The lower than expected damping is attributed to a manufacturing problem and will be corrected on the improved prototype.

Valve response times are acceptable for the current application.

The SIMULINK model of the suspension system gives acceptable results, but it will be updated in the next phase of the project to include heat transfer effects, smooth valve switching transitions and switching at any operation point.

5. Recommendations

The second phase of the project, as proposed in [25] should continue. Phase 2 of the project will focus on developing a complete vehicle model, validated against experimental results obtained from testing the baseline vehicle [26]. The vehicle model will be combined with the suspension model to simulate the whole system. Improvements and fine-tuning will be performed on the suspension hardware and a vehicle set will be manufactured. Phase 2 will consist of the following 7 tasks.

i) Complete (full) vehicle simulation model

A simulation model of a Landrover 110 sports utility vehicle (SUV) will be developed in ADAMS. The model will include detailed suspension kinematics, non-linear springs, dampers and bump stops as well as steering geometry. Best possible estimates for center of gravity height, moments of inertia and chassis torsional stiffness will be used.

ii) Baseline vehicle tests

A Landrover 110 SUV will be obtained locally for testing purposes. The vehicle will be evaluated for ride comfort over repeatable test tracks of various roughness at known, repeatable and representative speeds. Weighted RMS vertical accelerations will be used to quantify ride comfort. Vehicle handling will be evaluated using a severe double lane change maneuver as well as constant radius tests. Test procedures and the choice of terrains will be focused on ensuring repeatability. This is important as the baseline test results will be used during Phase 3 to quantify the improvements offered by the controllable suspension system.

iii) Validated vehicle model

The results obtained from the vehicle simulation model will be compared with results obtained during testing. The parameters in the vehicle model will be modified if necessary to obtain acceptable correlation.

iv) Mathematical models for suspension unit

The mathematical model for predicting the spring and damper characteristics (including valve response times) that was developed during Phase 1, will be

improved and incorporated into the vehicle model to enable future development of control systems in Phase 3.

v) Improved prototype

The existing prototype suspension will be improved to optimize characteristics, lower the mass, simplify the vehicle attachment points and mounting positions of the valves and accumulators. A prototype suspension unit will be manufactured according to the optimized design. Provision will be made to add ride height control at a later stage. The improved prototype will be characterized and tested to verify proper operation.

vi) Manufacture vehicle set

After successful testing of the improved prototype, a vehicle set of four suspension struts will be manufactured. The four struts will be tested to ensure conformance to the specification, and to detect premature failure due to seal damage during installation or manufacturing defects.

vii) Visit to TACOM

A visit to TACOM is planned to give feedback on the project progress as well as to discuss Phase 3 of the project.

The outputs of Phase 2 will be a vehicle set of suspension hardware, validated simulation model of the vehicle, as well as test and simulation reports.

6. Literature cited

[1] Van Rensburg, N., Steyn, J.L. and Els, P.S., **Time delay in a semi-active damper: modeling the bypass valve**, Journal of Terramechanics, Volume 39, 2002, pp. 35-45

[2] Giliomee, C.L. and Els, P.S., **Semi-Active Hydropneumatic Spring and Damper System**, Journal of Terramechanics, Volume 35, 1998, pp. 109-117

[3] Els, P.S. and Grobbelaar, B., **Investigation of the Time- and Temperature Dependency of Hydropneumatic Suspension Systems**, SAE Technical Paper Series no. 930265, Presented at the International Congress and Exposition, Detroit, Michigan, 1-5 March 1993

[4] Els, P.S. and Holman, T.J., **Development of a Semi-Active Rotary Damper for Armoured Fighting Vehicles**, Proceedings of the European Armoured Fighting Vehicle Symposium, 28-30 May 1996, Presented by Cranfield University and the Royal Military College of Science, Shrivenham, UK

[5] Els, P.S. and Grobbelaar, B., **Heat Transfer Effects on Hydropneumatic Suspension Systems**, In Proceedings of the 7th European ISTVS Conference, 8-10 October 1997, Ferrara, Italy, pp. 235-242

[6] Els, P.S. and Holman, T.J., **Semi-Active Rotary Damper for a Heavy Off-Road Wheeled Vehicle**, In Proceedings of the 7th European ISTVS Conference, 8-10 October 1997, Ferrara, Italy, pp. 259-266

[7] Giliomee, C.L. and Els, P.S., **Semi-Active Hydropneumatic Spring and Damper System**, In Proceedings of the 7th European ISTVS Conference, 8-10 October 1997, Ferrara, Italy, pp. 441-448

[8] Els, P.S. and Giliomee, C.L., **The Development History of Semi-Active Dampers in South Africa**, Proceedings of the Wheels and Tracks Symposium, Royal Military College of Science and Cranfield University, 9-11 September 1998

[9] Els, P.S. and Van Niekerk, J.L., **Dynamic Modelling of an Off-Road Vehicle for the Design of a Semi-Active, Hydropneumatic Spring-Damper System**, Proceedings of the 16th International Association for Vehicle System Dynamics (IAVSD) Symposium: Dynamics of Vehicles on roads and Tracks, Pretoria, South Africa, August 30 to September 3, 1999

[10] Els, P.S. and Nell, S., **Better Mobility for Armoured Vehicles - Developing a Semi-Active Rotary Damper**, SALVO - Armscor's Corporate Journal, 3/96, pp. 26-28.

[11] Els, P.S. and Grobbelaar, B., **Investigation of the Time- and Temperature Dependency of Hydropneumatic Suspension Systems**, SAE Technical Paper Series no. 930265, Published in Vehicle Suspension and Steering Systems, SAE Special Publication SP-256, 1993, pp. 55-65.

[12] Els, P.S. and Grobbelaar, B., **Heat Transfer Effects on Hydropneumatic Suspension Systems**, Submitted for publication in the Journal of Terramechanics.

[13] Giliomee, C.L. and Els, P.S., **Semi-Active Hydropneumatic Spring and Damper System**, Published in Journal of Terramechanics, Volume 35, 1998, pp. 109-117

[14] Els, P.S. and Holman, T.J., **Semi-Active Rotary Damper for a Heavy Off-Road Wheeled Vehicle**, Journal of Terramechanics, Volume 36, 1999, pp. 51-60

[15] Nell, S and Steyn J.L., **Experimental evaluation of an sophisticated two state semi-active damper**. Journal of Terramechanics, Vol. 31, no. 4, 1994, Elsevier Science Ltd.

[16] Nell, S and Steyn J.L., **An alternative control strategy for semi-active dampers on off-road vehicles**. Journal of Terramechanics, Vol. 35, 1998, pp 25-40.

[17] Nell, S and Steyn J.L., **Development and experimental evaluation of translational semi-active dampers on a high mobility off-road vehicle**. Submitted to Journal of Terramechanics.

[18] Nell S. and Steyn J.L., **Experimental evaluation of an unsophisticated two state semi-active damper**. International Society for Terrain Vehicle Systems. 11th International Conference. 1993, Nevada, USA. (Presented by Nell).

[19] Els, P.S., **TRIP REPORT : Discussions between Mr. P.S. Els (University of Pretoria) and Dr. F.B. Hoogterp (TACOM) regarding mutual research interests in the field of controllable suspension systems (29 August 2000).** Prepared for Dr. S.G. Sampath of the European Research Office, US Army. Report date : 12 September 2000, Reference : R&D 9041-AN-06

[20] Els, P.S., **Controllable Wheeled Vehicle Suspension Research,** Seed Project Proposal Submitted to European Research Office, USARDSG-UK, October 30, 2000

[21] Els, P.S. and Nell, S. **Ride Comfort Standards for Military Vehicles under Off-Road Conditions**, In Proceedings of the Wheels and Tracks Symposium, Royal Military College of Science and Cranfield University, 9-11 September 1998.

[22] Els, P.S. and Nell, S., **Comparison Between Subjective and Objective Ride Comfort for Military Off-Road Vehicles** , Proceedings of the 13th International Conference of the ISTVS, 14-17 September 1999, Munich, Germany.

[23] Els, P.S., **The Applicability of Ride Comfort Standards to Off-Road Vehicles,** Proceedings of the Human Response to Vibration, 34th Meeting of the UK Group, Ford Motor Company Limited, Dunton, Essex, UK, 22-24 September 1999.

[24] Naudé A.F. and Steyn J.L., **Objective evaluation of the simulated handling characteristics of a vehicle in a double lane change manoeuvre**. Society of Automotive Engineers Annual Congress. 1993, Detroit, USA. (Presented by Naudé).

[25] Snyman, J.A., **Report on TACOM/University of Pretoria meeting held on the 4th of June 2002 at TACOM, Detroit,** Report reference number: R&D 9345-AN-06, June, 2002

[26] Els, P.S., **Controllable Wheeled Vehicle Suspension Research – Phase 2,** Research Project Proposal Submitted to European Research Office, USARDSG-UK, June 20, 2002

[27] Els, P.S., and Visser-Uys, P.E., **Investigation Of The Applicability Of The Dynamic-Q Optimisation Algorithm To Vehicle Suspension Design,** Proceedings of the 4th ASMO-UK/ISSMO Conference: Engineering Design Optimisation – Product and Process Development, Newcastle-upon-Tyne, UK, 4 to 5 July 2002

[28] Genta, G., **Motor Vehicle Dynamics: Modeling and Simulation**, World Scientific, 1997

Appendix A

MATLAB Model

Ride Dynamics Model

Introduction

This appendix describes the derivation of the equations of motion used in a simulation program with a Runge-Kutta-type solver in MATLAB, for simulating the vehicle ride response of a Landrover Defender 110 sport utility vehicle. The program was developed to obtain a quick running simulation tool for the development of the suspension control system of a semi-active suspension system, specifically with respect to the vehicle ride. It was argued that for a more comprehensive simulation including both vehicle ride and handling, it would not be economically justifiable to develop such a model within the MATLAB environment, since multi-body dynamics programs such as DADS (Dynamic Analysis and Design System) or ADAMS provides a simulation facility that is much simpler to use, from a user point of view, than MATLAB.

The program described herein is based on equations of motion derived with Lagrangian dynamics, broadly in line with the methodology outlined by Genta [28, §6.3]. A simple point contact tire model is used. The suspension system kinematics are not modeled; instead simple assumptions are made that imply kinematic constraints determining the movement of the vehicle axles relative to the vehicle body. Small angle linearization is applied with respect to the rotation of rigid bodies, but the springs and dampers are modeled as fully non-linear elements.

Axis systems, definitions and assumptions

The axes systems as in [28, fig. 6.19, p. 360] are used: the X-Y-Z axis system is an inertial system (and the vector base system associated with this is referred to herein as the $\mathcal{I}$ base) while the x-y-z axis system is the axis system attached to the vehicle body (i.e. sprung mass) with its origin at the body center of mass (and the vector base system associated with this is referred to as the $\mathcal{B}$ base). The x axis points toward the front of the body, the y axis to the left and the z axis to the top. The symbols X, Y and Z are also used to describe the ***displacements*** of the body center of mass in the X-Y-Z axis system, i.e., the displacement vector of the body center of mass in the $\mathcal{I}$ base is $\lfloor\ X \quad Y \quad Z\ \rfloor^T$. Likewise, the displacement of the body center of mass in the $\mathcal{B}$ base is $\lfloor\ x \quad y \quad z\ \rfloor^T$. The displacement components of other points are distinguished form the center of mass displacement components through the use of subscripts. The same sequence of Euler angle rotations as employed by Genta on p. 360 is used here also, namely a yaw rotation ψ about the Z axis, followed by a pitch rotation θ about an intermediate y-axis, followed lastly by a roll rotation ϕ about the x axis.

The Landrover vehicle considered in this study has so-called rigid axles both front and rear. It is assumed that both these axles are kinematically constrained in such a way that their respective centers of mass, which are both assumed to lie in the $x-z$ plane, displace with the vectors $\lfloor\ x \quad y \quad z_f\ \rfloor^T$ and $\lfloor\ x \quad y \quad z_r\ \rfloor^T$ expressed in the $\mathcal{B}$ base, while the sequence of Euler angle rotations that applies to the body also applies to the two axles, except that the front and rear axles roll (the third Euler rotation) through angles ϕ_f and ϕ_r, respectively, instead of through the body roll angle of ϕ.

The wheels and corresponding suspension members are numbered as follows: 1 for left front, 2 for right front, 3 for left rear and 4 for right rear.

The following points and lengths are defined:

- Point c: the center of mass of the vehicle body (unsprung mass).

- Point d_i: the axle center of mass corresponding to the i-th wheel. This means that d_1 and d_2 are the same point, namely the center of mass of the front axle.
- Point e_i: a point attached to the vehicle body on an axis that is parallel to the z axis and in the x-z plane such that the axis contains point d_i. This means that e_1 and e_2 are the same point, namely the point determined by the front axle as described above.
- Length l_{0i}: the distance that e_i is above d_i (i.e., the difference in z coordinates between points e_i and point d_i, positive if e_i is above d_i) under static loading (when the vehicle is stationary on a horizontal surface with its weight on its wheels). If point e_i is chosen to be coincident with point d_i under static loading (i.e., as on a virtual extension of the vehicle body), $l_{0i} = 0$.
- Point g_i: the point of attachment to the corresponding axle of the spring-damper-combination corresponding to the i-th wheel.
- Point v_i: the point of attachment to the body of the spring-damper-combination corresponding to the i-th wheel.
- Point w_i: the center of the tire-ground contact area of wheel i.

Initially at $t = 0$ (i.e., before any rotation has taken place) the base vectors of the $\mathcal{I}$ base and the $\mathcal{B}$ base correspondingly coincide. The following position vectors are defined in the $\mathcal{B}$ base at $t = 0$:

- That of point e_i, relative to point c: $\lfloor\ l_{i_{e/c1}} \quad 0 \quad l_{i_{e/c3}}\ \rfloor^T$ (components constant with time)
- That of point v_i, relative to point e_i: $\lfloor\ 0 \quad l_{i_{v/e2}} \quad l_{i_{v/e3}}\ \rfloor^T$ (components constant with time)
- That of point g_i, relative to point d_i: $\lfloor\ 0 \quad l_{i_{g/d2}} \quad 0\ \rfloor^T$ (components vary with time)
- That of point w_i, relative to point d_i, with the vehicle under static loading conditions: $\lfloor\ 0 \quad l_{i_{w/d2}} \quad l_{i_{w/d3}}\ \rfloor^T$ (components vary with time).

Expressed in base $\mathcal{B}$, some of these vectors (those rotating together with the x-y-z axis system) will always remain the same, but in those cases where the vector does not rotate with the x-y-z axis system, its components will vary with time, as indicated above. Also note that the above definitions also imply assumptions on the positions where the spring-damper-combinations are attached to the axle units and the vehicle body.

The kinetic energy expression of especially the sprung mass is significantly simplified if the displacement components expressed in the $\mathcal{I}$ base are chosen as generalized coordinates, but then the expression for the potential energy is much more complicated. The analysis is simplified by assuming that both the vehicle body roll and pitch angles ϕ and θ remain small so that the sines of these angles may be approximated by the angles themselves, while their cosines may be approximated by one. Furthermore, since only a ride simulation will be performed, no lateral excitation is allowed and the yaw angle ψ and yaw rate $\dot{\psi}$ are both assumed to be constrained to zero. Under these assumptions, considering the motion of the axles relative to the vehicle body, the distinction between the actual motion which happens in the y-z-plane and an approximation to this motion which is assumed to take place in the Y-Z-plane becomes negligible. So, while earlier it was said that the axles are assumed to displace with the vectors $\lfloor\ x \quad y \quad z_f\ \rfloor^T$ and $\lfloor\ x \quad y \quad z_r\ \rfloor^T$ expressed in the $\mathcal{B}$ base, it is now assumed that these displacements are equally well described as the vectors $\lfloor\ X \quad Y \quad Z_f\ \rfloor^T$ and $\lfloor\ X \quad Y \quad Z_r\ \rfloor^T$ directly expressed in the $\mathcal{I}$ base, i.e., without transformation since the transformation matrix by approximation is an identity matrix.

The generalized coordinates q_i in which the dynamics of the problem is therefore described are Z, Z_f, Z_r, θ, ϕ, ϕ_f and ϕ_r. The vehicle is assumed to be constrained in its motion to ensure that the velocity component in the X direction remains constant and that Y and ψ always remain zero.

Potential Energy and Dissipation Functions

It should be noted that this appendix deviates from the convention adopted in the rest of the report in that in this appendix the spring displacements in compression and damper compression rates are taken as negative while spring displacements in extension and damper extension rates are taken as positive. In the same way, in this, the spring/damper forces are taken as positive when in tension and negative when in compression.

The elastic potential energy stored in the springs is given by:

$$U_S = U_{S1}(Z, Z_f, \phi, \theta, \phi_f) + U_{S2}(Z, Z_f, \phi, \theta, \phi_f) + U_{S3}(Z, Z_r, \phi, \theta, \phi_r) + U_{S4}(Z, Z_r, \phi, \theta, \phi_r)$$

where for the springs of the front axle, $i = 1, 2$:

$$U_{Si}(Z, Z_f, \phi, \theta, \phi_f) = U_{Si}(\Delta_i) \;\; ; \;\; \Delta_i = Z - Z_f - l_{i_{e/c1}}\theta + l_{i_{g/d2}}(\phi - \phi_f)$$

Δ_i being the extension of the i-th spring, while for the springs of the rear axle, $i = 3, 4$:

$$U_{Si}(Z, Z_r, \phi, \theta, \phi_r) = U_{Si}(\Delta_i) \;\; ; \;\; \Delta_i = Z - Z_r - l_{i_{e/c1}}\theta + l_{i_{g/d2}}(\phi - \phi_r)$$

Here it should be remembered that the expressions for Δ_i given above have been derived by linearizing the kinematics. Also,

$$\frac{\partial U_{Si}}{\partial q_i} = \frac{\partial U_{Si}}{\partial \Delta_i}\frac{\partial \Delta_i}{\partial q_i} = f_{Si}(\Delta_i)\frac{\partial \Delta_i}{\partial q_i}$$

where

$$f_{Si}(\Delta_i) = \frac{\partial U_{Si}}{\partial \Delta_i}$$

is the spring force (positive in tension; a non-linear function of Δ_i) in the i-th spring.

The elastic potential energy stored in the anti-roll bars is

$$U_{arb} = \frac{1}{2}k_{arb_f}(\phi - \phi_f)^2 + \frac{1}{2}k_{arb_r}(\phi - \phi_r)^2$$

The potential energy due to gravity is:

$$U_G = m_s g Z + m_f g Z_f + m_r g Z_r$$

The total potential energy is given by:

$$U = U_S + U_G$$

The Rayleigh dissipation function is given by:

$$\mathcal{F}_D = \mathcal{F}_{D1}(\dot{Z}, \dot{Z}_f, \dot{\phi}, \dot{\theta}, \dot{\phi}_f) + \mathcal{F}_{D2}(\dot{Z}, \dot{Z}_f, \dot{\phi}, \dot{\theta}, \dot{\phi}_f) + \mathcal{F}_{D3}(\dot{Z}, \dot{Z}_r, \dot{\phi}, \dot{\theta}, \dot{\phi}_r) + \mathcal{F}_{D4}(\dot{Z}, \dot{Z}_r, \dot{\phi}, \dot{\theta}, \dot{\phi}_r)$$

where for the dampers of the front axle ($i = 1, 2$):

$$\mathcal{F}_{Di}(\dot{Z}, \dot{Z}_f, \dot{\phi}, \dot{\theta}, \dot{\phi}_f) = \mathcal{F}_{Di}(\dot{\Delta}_i)$$

where for the dampers of the rear axle ($i = 3, 4$):

$$\mathcal{F}_{Di}(\dot{Z}, \dot{Z}_r, \dot{\phi}, \dot{\theta}, \dot{\phi}_r) = \mathcal{F}_{Di}(\dot{\Delta}_i)$$

where $\dot{\Delta}_i$ is the extension rate of the i-th damper, and when linearized, indeed,

$$\dot{\Delta}_i = \dot{Z} - \dot{Z}_f - l_{i_{e/c1}}\dot{\theta} + l_{i_{g/d2}}(\dot{\phi} - \dot{\phi}_f)$$

in the case of the front dampers and

$$\dot{\Delta}_i = \dot{Z} - \dot{Z}_r - l_{i_{c/c1}}\dot{\theta} + l_{i_{g/d2}}(\dot{\phi} - \dot{\phi}_r)$$

in the case of the rear. Also,

$$\frac{\partial \mathcal{F}_{Di}}{\partial \dot{q}_i} = \frac{\partial \mathcal{F}_{Di}}{\partial \dot{\Delta}_i}\frac{\partial \dot{\Delta}_i}{\partial \dot{q}_i} = f_{Di}(\dot{\Delta}_i)\frac{\partial \dot{\Delta}_i}{\partial \dot{q}_i}$$

where

$$f_{Di}(\dot{\Delta}_i) = \frac{\partial \mathcal{F}_{Di}}{\partial \dot{\Delta}_i}$$

is the damper force (positive in tension; a non-linear function of $\dot{\Delta}_i$) in the i-th damper.

The linearizing assumptions that were applied to derive the linear expressions for both Δ_i and $\dot{\Delta}_i$ are:

- The pitch and three roll angles θ, ϕ, ϕ_f and ϕ_r remain small such that the sine of any of these angles is by approximation the angle itself while the cosine is approximated by 1.
- The motion remains small (essentially a pertubational analysis) so that any terms containing products of generalized displacements or their time derivatives, of the nature $q_i q_j$, $q_i \dot{q}_j$ or $\dot{q}_i \dot{q}_j$, were ignored, compared to terms linear in these variables.
- $l_{i_{v/c2}} = l_{i_{g/d2}}$

Kinetic Energy

Using the same small angle assumption as above, Genta [28, p. 361, 362] derives the following expression for the angular velocity of the vehicle body, expressed in the $\mathcal{B}$ base, in terms of the roll, pitch and yaw angles and rates:

$$\underline{\omega}^* = \left\{ \begin{array}{c} p \\ q \\ r \end{array} \right\} = \left\{ \begin{array}{c} \dot{\phi} - \theta\dot{\psi} \\ \dot{\theta} + \phi\dot{\psi} \\ \dot{\psi} - \phi\dot{\theta} \end{array} \right\}$$

Substituting the additional assumption that the yaw rate is also zero in the above leads to

$$\underline{\omega}^* = \left\{ \begin{array}{c} p \\ q \\ r \end{array} \right\} = \left\{ \begin{array}{c} \dot{\phi} \\ \dot{\theta} \\ -\phi\dot{\theta} \end{array} \right\}$$

In deriving the kinetic energy, the same approach is followed as in Genta [28, p. 363]. Here, however, a further simplifying assumption is made that the vehicle body product of inertia J_{xz} in the vehicle body axis is also zero, leading to a diagonal inertia tensor in the $\mathcal{B}$ base. This assumption is perhaps not fully justified, since neither the x nor the z axes of the body are axes of symmetry. In the case of the Landrover, however, this assumption is not too bad either. With respect to both the front and rear axles it is assumed that the moment of inertia of the axle about the axle axis (i.e., the y-axis) is negligibly small, compared to that of the vehicle body. Furthermore, it is assumed that the moments of inertia about the other two axes x and z are approximately the same, J_f in the front and J_r in the rear, and that these are the principle moments of inertia of the axle units. The kinetic energy of the whole vehicle

is then given by approximation by:

$$
\begin{aligned}
T &= \frac{1}{2}m_s(\dot{X}^2+\dot{Z}^2)+\frac{1}{2}\left\{\begin{array}{c}\dot{\phi}\\ \dot{\theta}\\ -\phi\dot{\theta}\end{array}\right\}^T\left[\begin{array}{ccc}J_x & 0 & 0\\ 0 & J_y & 0\\ 0 & 0 & J_z\end{array}\right]\left\{\begin{array}{c}\dot{\phi}\\ \dot{\theta}\\ -\phi\dot{\theta}\end{array}\right\}\\
&\quad+\frac{1}{2}m_f(\dot{X}^2+\dot{Z}_f^2)+\frac{1}{2}\left\{\begin{array}{c}\dot{\phi}_f\\ \dot{\theta}\\ -\phi_f\dot{\theta}\end{array}\right\}^T\left[\begin{array}{ccc}J_f & 0 & 0\\ 0 & 0 & 0\\ 0 & 0 & J_f\end{array}\right]\left\{\begin{array}{c}\dot{\phi}_f\\ \dot{\theta}\\ -\phi_f\dot{\theta}\end{array}\right\}\\
&\quad+\frac{1}{2}m_r(\dot{X}^2+\dot{Z}_r^2)+\frac{1}{2}\left\{\begin{array}{c}\dot{\phi}_r\\ \dot{\theta}\\ -\phi_r\dot{\theta}\end{array}\right\}^T\left[\begin{array}{ccc}J_r & 0 & 0\\ 0 & 0 & 0\\ 0 & 0 & J_r\end{array}\right]\left\{\begin{array}{c}\dot{\phi}_r\\ \dot{\theta}\\ -\phi_r\dot{\theta}\end{array}\right\}\\
&= \frac{1}{2}m_s(\dot{X}^2+\dot{Z}^2)+\frac{1}{2}J_x\dot{\phi}^2+\frac{1}{2}J_y\dot{\theta}^2+\frac{1}{2}J_z\phi^2\dot{\theta}^2\\
&\quad+\frac{1}{2}m_f(\dot{X}^2+\dot{Z}_f^2)+\frac{1}{2}J_f\dot{\phi}_f^2+\frac{1}{2}J_f\phi_f^2\dot{\theta}^2+\frac{1}{2}m_r(\dot{X}^2+\dot{Z}_r^2)+\frac{1}{2}J_r\dot{\phi}_r^2+\frac{1}{2}J_r\phi_r^2\dot{\theta}^2
\end{aligned}
$$

Virtual Work done by External Forces

Virtual work done by forces on front wheel i $(i=1,2)$ is:

$$\delta W_{wi} = f_{wiz}(\delta Z_f + l_{i_{w/d2}}\delta\phi_f)$$

Virtual work done by forces on rear wheel i $(i=3,4)$ is:

$$\delta W_{wi} = f_{wiz}(\delta Z_r + l_{i_{w/d2}}\delta\phi_r)$$

Virtual work done by external forces:

$$\delta W = \sum_{i=1}^{4}\delta W_{wi}$$

Equations of Motion

Lagrange's equations are now derived using

$$\frac{d}{dt}\frac{\partial T}{\partial\dot{q}_i}-\frac{\partial T}{\partial q_i}+\frac{\partial U}{\partial q_i}+\frac{\partial\mathcal{F}}{\partial\dot{q}_i}=Q_i$$

where $Q_i=\dfrac{\partial(\delta W)}{\partial\delta q_i}$.

Equation of motion w.r.t. generalized coordinate Z

$$\frac{\partial T}{\partial \dot{Z}} = m_s \dot{Z}$$

$$\therefore \quad \frac{d}{dt}\frac{\partial T}{\partial \dot{Z}} = m_s \ddot{Z}$$

$$\frac{\partial T}{\partial Z} = 0$$

$$\begin{aligned}\frac{\partial U}{\partial Z} &= \frac{\partial U_{S1}}{\partial Z} + \frac{\partial U_{S2}}{\partial Z} + \frac{\partial U_{S3}}{\partial Z} + \frac{\partial U_{S1}}{\partial Z} + \frac{\partial U_G}{\partial Z} \\ &= f_{S1}(Z, Z_f, \phi, \theta, \phi_f) + f_{S2}(Z, Z_f, \phi, \theta, \phi_f) + f_{S3}(Z, Z_r, \phi, \theta, \phi_r) + f_{S4}(Z, Z_r, \phi, \theta, \phi_r) + m_s g\end{aligned}$$

$$\begin{aligned}\frac{\partial \mathcal{F}}{\partial \dot{Z}} &= \frac{\mathcal{F}_{D1}}{\partial \dot{Z}} + \frac{\mathcal{F}_{D2}}{\partial \dot{Z}} + \frac{\mathcal{F}_{D3}}{\partial \dot{Z}} + \frac{\mathcal{F}_{D4}}{\partial \dot{Z}} \\ &= f_{D1}(\dot{Z}, \dot{Z}_f, \dot{\phi}, \dot{\theta}, \dot{\phi}_f) + f_{D2}(\dot{Z}, \dot{Z}_f, \dot{\phi}, \dot{\theta}, \dot{\phi}_f) + f_{D3}(\dot{Z}, \dot{Z}_r, \dot{\phi}, \dot{\theta}, \dot{\phi}_r) + f_{D4}(\dot{Z}, \dot{Z}_r, \dot{\phi}, \dot{\theta}, \dot{\phi}_r)\end{aligned}$$

$$Q_z = \frac{\partial}{\partial \delta Z}(\delta W) = 0$$

$$\begin{aligned}&\therefore \quad m_s \ddot{Z} + f_{S1}(Z, Z_f, \phi, \theta, \phi_f) + f_{S2}(Z, Z_f, \phi, \theta, \phi_f) + f_{S3}(Z, Z_r, \phi, \theta, \phi_r) + f_{S4}(Z, Z_r, \phi, \theta, \phi_r) \\ &+ m_s g + f_{D1}(\dot{Z}, \dot{Z}_f, \dot{\phi}, \dot{\theta}, \dot{\phi}_f) + f_{D2}(\dot{Z}, \dot{Z}_f, \dot{\phi}, \dot{\theta}, \dot{\phi}_f) + f_{D3}(\dot{Z}, \dot{Z}_r, \dot{\phi}, \dot{\theta}, \dot{\phi}_r) + f_{D4}(\dot{Z}, \dot{Z}_r, \dot{\phi}, \dot{\theta}, \dot{\phi}_r) = 0\end{aligned}$$

Equation of motion w.r.t. generalized coordinate Z_f

$$\frac{\partial T}{\partial \dot{Z}_f} = m_f \dot{Z}_f$$

$$\therefore \quad \frac{d}{dt}\frac{\partial T}{\partial \dot{Z}_f} = m_f \ddot{Z}_f$$

$$\frac{\partial T}{\partial Z_f} = 0$$

$$\begin{aligned}\frac{\partial U}{\partial Z_f} &= \frac{\partial U_{S1}}{\partial Z_f} + \frac{\partial U_{S2}}{\partial Z_f} + \frac{\partial U_G}{\partial Z_f} \\ &= -f_{S1}(Z, Z_f, \phi, \theta, \phi_f) - f_{S2}(Z, Z_f, \phi, \theta, \phi_f) + m_f g\end{aligned}$$

$$\frac{\partial \mathcal{F}}{\partial \dot{Z}_f} = \frac{\mathcal{F}_{D1}}{\partial \dot{Z}_f} + \frac{\mathcal{F}_{D2}}{\partial \dot{Z}_f}$$

$$= -f_{D1}(\dot{Z}, \dot{Z}_f, \dot{\phi}, \dot{\theta}, \dot{\phi}_f) - f_{D2}(\dot{Z}, \dot{Z}_f, \dot{\phi}, \dot{\theta}, \dot{\phi}_f)$$

$$Q_{Z_f} = \frac{\partial}{\partial \delta Z_f}(\delta W) = f_{w1z} + f_{w2z}$$

$$\therefore \quad m_f \ddot{Z}_f - f_{S1}(Z, Z_f, \phi, \theta, \phi_f) - f_{S2}(Z, Z_f, \phi, \theta, \phi_f) + m_f g$$
$$- f_{D1}(\dot{Z}, \dot{Z}_f, \dot{\phi}, \dot{\theta}, \dot{\phi}_f) - f_{D2}(\dot{Z}, \dot{Z}_f, \dot{\phi}, \dot{\theta}, \dot{\phi}_f) = f_{w1z} + f_{w2z}$$

Equation of motion w.r.t. generalized coordinate Z_r

$$\frac{\partial T}{\partial \dot{Z}_r} = m_r \dot{Z}_r$$

$$\therefore \quad \frac{d}{dt}\frac{\partial T}{\partial \dot{Z}_r} = m_r \ddot{Z}_r$$

$$\frac{\partial T}{\partial Z_r} = 0$$

$$\frac{\partial U}{\partial Z_r} = \frac{\partial U_{S3}}{\partial Z_r} + \frac{\partial U_{S4}}{\partial Z_r} + \frac{\partial U_G}{\partial Z_r}$$

$$= -f_{S3}(Z, Z_r, \phi, \theta, \phi_r) - f_{S4}(Z, Z_r, \phi, \theta, \phi_r) + m_r g$$

$$\frac{\partial \mathcal{F}}{\partial \dot{Z}_r} = \frac{\mathcal{F}_{D3}}{\partial \dot{Z}_r} + \frac{\mathcal{F}_{D4}}{\partial \dot{Z}_r}$$

$$= -f_{D3}(\dot{Z}, \dot{Z}_r, \dot{\phi}, \dot{\theta}, \dot{\phi}_r) - f_{D4}(\dot{Z}, \dot{Z}_r, \dot{\phi}, \dot{\theta}, \dot{\phi}_r)$$

$$Q_{Z_r} = \frac{\partial}{\partial \delta Z_r}(\delta W) = f_{w3z} + f_{w4z}$$

$$\therefore \quad m_r \ddot{Z}_r - f_{S3}(Z, Z_r, \phi, \theta, \phi_r) - f_{S4}(Z, Z_r, \phi, \theta, \phi_r) + m_r g$$
$$- f_{D3}(\dot{Z}, \dot{Z}_r, \dot{\phi}, \dot{\theta}, \dot{\phi}_r) - f_{D4}(\dot{Z}, \dot{Z}_r, \dot{\phi}, \dot{\theta}, \dot{\phi}_r) = f_{w3z} + f_{w4z}$$

Equation of motion w.r.t. generalized coordinate θ

$$\frac{\partial T}{\partial \dot{\theta}} = J_y\dot{\theta} + J_z\phi^2\dot{\theta} + J_f\phi_f^2\dot{\theta} + J_r\phi_r^2\dot{\theta}$$

$$\begin{aligned}\therefore \quad \frac{d}{dt}\frac{\partial T}{\partial \dot{\theta}} &= J_y\ddot{\theta} + J_z(\phi^2\ddot{\theta} + 2\phi\dot{\phi}\dot{\theta}) + J_f(\phi_f^2\ddot{\theta} + 2\phi_f\dot{\phi}_f\dot{\theta}) + J_r(\phi_r^2\ddot{\theta} + 2\phi_r\dot{\phi}_r\dot{\theta}) \\ &\approx J_y\ddot{\theta} + 2J_z\phi\dot{\phi}\dot{\theta} + 2J_f\phi_f\dot{\phi}_f\dot{\theta} + 2J_r\phi_r\dot{\phi}_r\dot{\theta}\end{aligned}$$

where the terms in ϕ^2, ϕ_f^2 and ϕ_r^2 have been neglected since roll angles ϕ, ϕ_f and ϕ_r are assumed to be small.

$$\frac{\partial T}{\partial \theta} = 0$$

$$\begin{aligned}\frac{\partial U}{\partial \theta} &= \frac{\partial U_{S1}}{\partial \theta} + \frac{\partial U_{S2}}{\partial \theta} + \frac{\partial U_{S3}}{\partial \theta} + \frac{\partial U_{S4}}{\partial \theta} \\ &= -l_{1_{e/c1}} f_{S1}(Z, Z_f, \phi, \theta, \phi_f) - l_{2_{e/c1}} f_{S2}(Z, Z_f, \phi, \theta, \phi_f) \\ &\quad - l_{3_{e/c1}} f_{S3}(Z, Z_r, \phi, \theta, \phi_r) - l_{4_{e/c1}} f_{S4}(Z, Z_r, \phi, \theta, \phi_r)\end{aligned}$$

$$\begin{aligned}\frac{\partial \mathcal{F}}{\partial \dot{\theta}} &= \frac{\mathcal{F}_{D1}}{\partial \dot{\theta}} + \frac{\mathcal{F}_{D2}}{\partial \dot{\theta}} + \frac{\mathcal{F}_{D3}}{\partial \dot{\theta}} + \frac{\mathcal{F}_{D4}}{\partial \dot{\theta}} \\ &= -l_{1_{e/c1}} f_{D1}(\dot{Z}, \dot{Z}_f, \dot{\phi}, \theta, \dot{\phi}_f) - l_{2_{e/c1}} f_{D2}(\dot{Z}, \dot{Z}_f, \dot{\phi}, \theta, \dot{\phi}_f) \\ &\quad - l_{3_{e/c1}} f_{D3}(\dot{Z}, \dot{Z}_r, \dot{\phi}, \theta, \dot{\phi}_r) - l_{4_{e/c1}} f_{D4}(\dot{Z}, \dot{Z}_r, \dot{\phi}, \theta, \dot{\phi}_r)\end{aligned}$$

$$Q_\theta = 0$$

$$\begin{aligned}\therefore \quad & J_y\ddot{\theta} + 2J_z\phi\dot{\phi}\dot{\theta} + 2J_f\phi_f\dot{\phi}_f\dot{\theta} + 2J_r\phi_r\dot{\phi}_r\dot{\theta} - l_{1_{e/c1}} f_{S1}(Z, Z_f, \phi, \theta, \phi_f) - l_{2_{e/c1}} f_{S2}(Z, Z_f, \phi, \theta, \phi_f) \\ & - l_{3_{e/c1}} f_{S3}(Z, Z_r, \phi, \theta, \phi_r) - l_{4_{e/c1}} f_{S4}(Z, Z_r, \phi, \theta, \phi_r) - l_{1_{e/c1}} f_{D1}(\dot{Z}, \dot{Z}_f, \dot{\phi}, \dot{\theta}, \dot{\phi}_f) \\ & - l_{2_{e/c1}} f_{D2}(\dot{Z}, \dot{Z}_f, \dot{\phi}, \dot{\theta}, \dot{\phi}_f) - l_{3_{e/c1}} f_{D3}(\dot{Z}, \dot{Z}_r, \dot{\phi}, \dot{\theta}, \dot{\phi}_r) - l_{4_{e/c1}} f_{D4}(\dot{Z}, \dot{Z}_r, \dot{\phi}, \dot{\theta}, \dot{\phi}_r) = 0\end{aligned}$$

Equation of motion w.r.t. generalized coordinate ϕ

$$\frac{\partial T}{\partial \dot{\phi}} = J_x\dot{\phi}$$

$$\therefore \quad \frac{d}{dt}\frac{\partial T}{\partial \dot{\phi}} = J_x\ddot{\phi}$$

$$\frac{\partial T}{\partial \phi} = J_z \phi \dot{\theta}^2$$

$$\therefore \quad \frac{d}{dt}\frac{\partial T}{\partial \dot{\phi}} - \frac{\partial T}{\partial \phi} = J_x \ddot{\phi} - J_z \phi \dot{\theta}^2$$

$$\begin{aligned}
\frac{\partial U}{\partial \phi} &= \frac{\partial U_{S1}}{\partial \phi} + \frac{\partial U_{S2}}{\partial \phi} + \frac{\partial U_{S3}}{\partial \phi} + \frac{\partial U_{S4}}{\partial \phi} + \frac{\partial U_{arb}}{\partial \phi} \\
&= l_{1_{g/d2}} f_{S1}(Z, Z_f, \phi, \theta, \phi_f) + l_{2_{g/d2}} f_{S2}(Z, Z_f, \phi, \theta, \phi_f) + k_{arb_f}(\phi - \phi_f) \\
&\quad + l_{3_{g/d2}} f_{S3}(Z, Z_r, \phi, \theta, \phi_r) + l_{4_{g/d2}} f_{S4}(Z, Z_r, \phi, \theta, \phi_r) + k_{arb_r}(\phi - \phi_r)
\end{aligned}$$

$$\begin{aligned}
\frac{\partial \mathcal{F}}{\partial \dot{\phi}} &= \frac{\mathcal{F}_{D1}}{\partial \dot{\phi}} + \frac{\mathcal{F}_{D2}}{\partial \dot{\phi}} + \frac{\mathcal{F}_{D3}}{\partial \dot{\phi}} + \frac{\mathcal{F}_{D4}}{\partial \dot{\phi}} \\
&= l_{1_{g/d2}} f_{D1}(\dot{Z}, \dot{Z}_f, \dot{\phi}, \dot{\theta}, \dot{\phi}_f) + l_{2_{g/d2}} f_{D2}(\dot{Z}, \dot{Z}_f, \dot{\phi}, \dot{\theta}, \dot{\phi}_f) \\
&\quad + l_{3_{g/d2}} f_{D3}(\dot{Z}, \dot{Z}_r, \dot{\phi}, \dot{\theta}, \dot{\phi}_r) + l_{4_{g/d2}} f_{D4}(\dot{Z}, \dot{Z}_r, \dot{\phi}, \dot{\theta}, \dot{\phi}_r)
\end{aligned}$$

$$Q_\phi = 0$$

$$\begin{aligned}
&\therefore \quad J_x \ddot{\phi} - J_z \phi \dot{\theta}^2 + l_{1_{g/d2}} f_{S1}(Z, Z_f, \phi, \theta, \phi_f) \\
&+ l_{2_{g/d2}} f_{S2}(Z, Z_f, \phi, \theta, \phi_f) + l_{3_{g/d2}} f_{S3}(Z, Z_r, \phi, \theta, \phi_r) + l_{4_{g/d2}} f_{S4}(Z, Z_r, \phi, \theta, \phi_r) \\
&+ l_{1_{g/d2}} f_{D1}(\dot{Z}, \dot{Z}_f, \dot{\phi}, \dot{\theta}, \dot{\phi}_f) + l_{2_{g/d2}} f_{D2}(\dot{Z}, \dot{Z}_f, \dot{\phi}, \dot{\theta}, \dot{\phi}_f) + l_{3_{g/d2}} f_{D3}(\dot{Z}, \dot{Z}_r, \dot{\phi}, \dot{\theta}, \dot{\phi}_r) \\
&+ l_{4_{g/d2}} f_{D4}(\dot{Z}, \dot{Z}_r, \dot{\phi}, \dot{\theta}, \dot{\phi}_r) + k_{arb_f}(\phi - \phi_f) + k_{arb_r}(\phi - \phi_r) = 0
\end{aligned}$$

Equation of motion w.r.t. generalized coordinate ϕ_f

$$\frac{\partial T}{\partial \dot{\phi}_f} = J_f \dot{\phi}_f$$

$$\therefore \quad \frac{d}{dt}\frac{\partial T}{\partial \dot{\phi}_f} = J_f \ddot{\phi}_f$$

$$\frac{\partial T}{\partial \phi_f} = J_f \phi_f \dot{\theta}^2$$

$$\therefore \quad \frac{d}{dt}\frac{\partial T}{\partial \dot{\phi}_f} - \frac{\partial T}{\partial \phi_f} = J_f(\ddot{\phi}_f - \phi_f \dot{\theta}^2)$$

$$\frac{\partial U}{\partial \phi_f} = \frac{\partial U_{S1}}{\partial \phi_f} + \frac{\partial U_{S2}}{\partial \phi_f} + \frac{\partial U_{arb}}{\partial \phi_f}$$

$$= -l_{1_{g/d2}} f_{S1}(Z, Z_f, \phi, \theta, \phi_f) - l_{2_{g/d2}} f_{S2}(Z, Z_f, \phi, \theta, \phi_f)$$

$$- k_{arb_f}(\phi - \phi_f)$$

$$\frac{\partial \mathcal{F}}{\partial \dot{\phi}_f} = \frac{\mathcal{F}_{D1}}{\partial \dot{\phi}_f} + \frac{\mathcal{F}_{D2}}{\partial \dot{\phi}_f}$$

$$= -l_{1_{g/d2}} f_{D1}(\dot{Z}, \dot{Z}_f, \dot{\phi}, \dot{\theta}, \dot{\phi}_f) - l_{2_{g/d2}} f_{D2}(\dot{Z}, \dot{Z}_f, \dot{\phi}, \dot{\theta}, \dot{\phi}_f)$$

$$Q_{\phi_f} = \frac{\partial}{\partial \delta \phi_f}(\delta W) = \sum_{i=1}^{2} f_{wiz} l_{i_{w/d2}}$$

$$\therefore \quad J_f(\ddot{\phi}_f - \phi_f \dot{\theta}^2) - l_{1_{g/d2}} f_{S1}(Z, Z_f, \phi, \theta, \phi_f) - l_{2_{g/d2}} f_{S2}(Z, Z_f, \phi, \theta, \phi_f)$$

$$- l_{1_{g/d2}} f_{D1}(\dot{Z}, \dot{Z}_f, \dot{\phi}, \dot{\theta}, \dot{\phi}_f) - l_{2_{g/d2}} f_{D2}(\dot{Z}, \dot{Z}_f, \dot{\phi}, \dot{\theta}, \dot{\phi}_f) - k_{arb_f}(\phi - \phi_f) = \sum_{i=1}^{2} f_{wiz} l_{i_{w/d2}}$$

Equation of motion w.r.t. generalized coordinate ϕ_r

$$\frac{\partial T}{\partial \dot{\phi}_r} = J_r \dot{\phi}_r$$

$$\therefore \quad \frac{d}{dt}\frac{\partial T}{\partial \dot{\phi}_r} = J_r \ddot{\phi}_r$$

$$\frac{\partial T}{\partial \phi_r} = J_r \phi_r \dot{\theta}^2$$

$$\therefore \quad \frac{d}{dt}\frac{\partial T}{\partial \dot{\phi}_r} - \frac{\partial T}{\partial \phi_r} = J_r(\ddot{\phi}_r - \phi_r \dot{\theta}^2)$$

$$\frac{\partial U}{\partial \phi_r} = \frac{\partial U_{S3}}{\partial \phi_r} + \frac{\partial U_{S4}}{\partial \phi_r} + \frac{\partial U_{arb}}{\partial \phi_r}$$

$$= -l_{3_{g/d2}} f_{S3}(Z, Z_r, \phi, \theta, \phi_r) - l_{4_{g/d2}} f_{S4}(Z, Z_r, \phi, \theta, \phi_r)$$

$$- k_{arb_r}(\phi - \phi_r)$$

$$\frac{\partial \mathcal{F}}{\partial \dot{\phi}_r} = \frac{\mathcal{F}_{D3}}{\partial \dot{\phi}_r} + \frac{\mathcal{F}_{D4}}{\partial \dot{\phi}_r}$$

$$= -l_{3_{g/d2}} f_{D3}(\dot{Z}, \dot{Z}_r, \dot{\phi}, \dot{\theta}, \dot{\phi}_r) - l_{4_{g/d2}} f_{D4}(\dot{Z}, \dot{Z}_r, \dot{\phi}, \dot{\theta}, \dot{\phi}_r)$$

$$Q_{\phi_r} = \frac{\partial}{\partial \delta \phi_r}(\delta W) = \sum_{i=3}^{4} f_{wiz} l_{i_{w/d2}}$$

$$\therefore \quad J_r(\ddot{\phi}_r - \phi_r\dot{\theta}^2) - l_{3_{g/d2}} f_{S3}(Z, Z_r, \phi, \theta, \phi_r) - l_{4_{g/d2}} f_{S4}(Z, Z_r, \phi, \theta, \phi_r)$$

$$- l_{3_{g/d2}} f_{D3}(\dot{Z}, \dot{Z}_r, \dot{\phi}, \dot{\theta}, \dot{\phi}_r) - l_{4_{g/d2}} f_{D4}(\dot{Z}, \dot{Z}_r, \dot{\phi}, \dot{\theta}, \dot{\phi}_r) - k_{arb_r}(\phi - \phi_r) \quad = \quad \sum_{i=3}^{4} f_{wiz} l_{i_{w/d2}}$$

Let the state vector be defined as

$$\underline{q} = \lfloor \; Z \quad Z_f \quad Z_r \quad \theta \quad \phi \quad \phi_f \quad \phi_r \quad \dot{Z} \quad \dot{Z}_f \quad \dot{Z}_r \quad \dot{\theta} \quad \dot{\phi} \quad \dot{\phi}_f \quad \dot{\phi}_r \; \rfloor^T$$

Then the above 7 equations of motion may be summarized as follows:

$$M\dot{\underline{q}} = \underline{F}(\underline{q}, \underline{f}_w) \tag{A1}$$

where $\underline{F}$ is a nonlinear column vector function of the state vector and the wheel force vector $\underline{f}_w$, which contains the vertical components of the wheel forces. The matrix M is given by

$$M = \begin{bmatrix} I_7 & [0]_7 \\ [0]_7 & M_{[22]} \end{bmatrix}$$

where I_7 and $[0]_7$ are a 7×7 identity and zero matrix, respectively, and where the 7×7 submatrix $M_{[22]}$ is given by:

$$M_{[22]} = \begin{bmatrix} m_s & 0 & 0 & 0 & 0 & 0 & 0 \\ 0 & m_f & 0 & 0 & 0 & 0 & 0 \\ 0 & 0 & m_r & 0 & 0 & 0 & 0 \\ 0 & 0 & 0 & J_y & 0 & 0 & 0 \\ 0 & 0 & 0 & 0 & J_x & 0 & 0 \\ 0 & 0 & 0 & 0 & 0 & J_f & 0 \\ 0 & 0 & 0 & 0 & 0 & 0 & J_r \end{bmatrix}$$

Thus it is seen that the matrix M is diagonal.

If $\underline{F}$ is divided into two 7×1 sub-vectors $\underline{F}_{[1]}$ and $\underline{F}_{[2]}$, such that $\underline{F}^T = \lfloor \; \underline{F}_{[1]}^T \quad \underline{F}_{[2]}^T \; \rfloor$, then

$$\underline{F}_{[1]} = \begin{bmatrix} [0]_7 & I_7 \end{bmatrix} \underline{q}$$

while the column vector $\underline{F}_{[2]}$ is given as follows:

1st row:

$$- f_{S1}(Z, Z_f, \phi, \theta, \phi_f) - f_{S2}(Z, Z_f, \phi, \theta, \phi_f) - f_{S3}(Z, Z_r, \phi, \theta, \phi_r) - f_{S4}(Z, Z_r, \phi, \theta, \phi_r) - m_s g$$
$$- f_{D1}(\dot{Z}, \dot{Z}_f, \dot{\phi}, \dot{\theta}, \dot{\phi}_f) - f_{D2}(\dot{Z}, \dot{Z}_f, \dot{\phi}, \dot{\theta}, \dot{\phi}_f) - f_{D3}(\dot{Z}, \dot{Z}_r, \dot{\phi}, \dot{\theta}, \dot{\phi}_r) - f_{D4}(\dot{Z}, \dot{Z}_r, \dot{\phi}, \dot{\theta}, \dot{\phi}_r)$$

2nd row:

$$f_{S1}(Z, Z_f, \phi, \theta, \phi_f) + f_{S2}(Z, Z_f, \phi, \theta, \phi_f) - m_f g$$
$$+ f_{D1}(\dot{Z}, \dot{Z}_f, \dot{\phi}, \dot{\theta}, \dot{\phi}_f) + f_{D2}(\dot{Z}, \dot{Z}_f, \dot{\phi}, \dot{\theta}, \dot{\phi}_f) + f_{w1z} + f_{w2z}$$

3rd row:

$$f_{S3}(Z, Z_r, \phi, \theta, \phi_r) + f_{S4}(Z, Z_r, \phi, \theta, \phi_r) - m_r g$$
$$+ f_{D3}(\dot{Z}, \dot{Z}_r, \dot{\phi}, \dot{\theta}, \dot{\phi}_r) + f_{D4}(\dot{Z}, \dot{Z}_r, \dot{\phi}, \dot{\theta}, \dot{\phi}_r) + f_{w3z} + f_{w4z}$$

4th row:

$$-2J_z\phi\dot{\phi}\dot{\theta} - 2J_f\phi_f\dot{\phi}_f\dot{\theta} - 2J_r\phi_r\dot{\phi}_r\dot{\theta} + l_{1_{e/c1}}f_{S1}(Z, Z_f, \phi, \theta, \phi_f) + l_{2_{e/c1}}f_{S2}(Z, Z_f, \phi, \theta, \phi_f)$$
$$+ l_{3_{e/c1}}f_{S3}(Z, Z_r, \phi, \theta, \phi_r) + l_{4_{e/c1}}f_{S4}(Z, Z_r, \phi, \theta, \phi_r) + l_{1_{e/c1}}f_{D1}(\dot{Z}, \dot{Z}_f, \dot{\phi}, \dot{\theta}, \dot{\phi}_f)$$
$$+ l_{2_{e/c1}}f_{D2}(\dot{Z}, \dot{Z}_f, \dot{\phi}, \dot{\theta}, \dot{\phi}_f) + l_{3_{e/c1}}f_{D3}(\dot{Z}, \dot{Z}_r, \dot{\phi}, \dot{\theta}, \dot{\phi}_r) + l_{4_{e/c1}}f_{D4}(\dot{Z}, \dot{Z}_r, \dot{\phi}, \dot{\theta}, \dot{\phi}_r)$$

5th row:

$$J_z\phi\dot{\theta}^2 - l_{1_{g/d2}}f_{S1}(Z, Z_f, \phi, \theta, \phi_f)$$
$$- l_{2_{g/d2}}f_{S2}(Z, Z_f, \phi, \theta, \phi_f) - l_{3_{g/d2}}f_{S3}(Z, Z_r, \phi, \theta, \phi_r) - l_{4_{g/d2}}f_{S4}(Z, Z_r, \phi, \theta, \phi_r)$$
$$- l_{1_{g/d2}}f_{D1}(\dot{Z}, \dot{Z}_f, \dot{\phi}, \dot{\theta}, \dot{\phi}_f) - l_{2_{g/d2}}f_{D2}(\dot{Z}, \dot{Z}_f, \dot{\phi}, \dot{\theta}, \dot{\phi}_f) - l_{3_{g/d2}}f_{D3}(\dot{Z}, \dot{Z}_r, \dot{\phi}, \dot{\theta}, \dot{\phi}_r)$$
$$- l_{4_{g/d2}}f_{D4}(\dot{Z}, \dot{Z}_r, \dot{\phi}, \dot{\theta}, \dot{\phi}_r) - k_{arb_f}(\phi - \phi_f) - k_{arb_r}(\phi - \phi_r)$$

6th row:

$$J_f\phi_f\dot{\theta}^2 + l_{1_{g/d2}}f_{S1}(Z, Z_f, \phi, \theta, \phi_f) + l_{2_{g/d2}}f_{S2}(Z, Z_f, \phi, \theta, \phi_f) + l_{1_{g/d2}}f_{D1}(\dot{Z}, \dot{Z}_f, \dot{\phi}, \dot{\theta}, \dot{\phi}_f)$$
$$+ l_{2_{g/d2}}f_{D2}(\dot{Z}, \dot{Z}_f, \dot{\phi}, \dot{\theta}, \dot{\phi}_f) + k_{arb_f}(\phi - \phi_f) + \sum_{i=1}^{2} f_{wiz}l_{i_{w/d2}}$$

7th row:

$$J_r\phi_r\dot{\theta}^2 + l_{3_{g/d2}}f_{S3}(Z, Z_r, \phi, \theta, \phi_r) + l_{4_{g/d2}}f_{S4}(Z, Z_r, \phi, \theta, \phi_r) + l_{3_{g/d2}}f_{D3}(\dot{Z}, \dot{Z}_r, \dot{\phi}, \dot{\theta}, \dot{\phi}_r)$$
$$+ l_{4_{g/d2}}f_{D4}(\dot{Z}, \dot{Z}_r, \dot{\phi}, \dot{\theta}, \dot{\phi}_r) + k_{arb_r}(\phi - \phi_r) + \sum_{i=3}^{4} f_{wiz}l_{i_{w/d2}}$$

The equation (A1) is recognized as a first order differential equation in a form that MATLAB can solve using its built in Runge-Kutta solvers.

Appendix B

Basic Dimensions of Prototype Suspension Unit

(All dimensions in mm – do not scale)

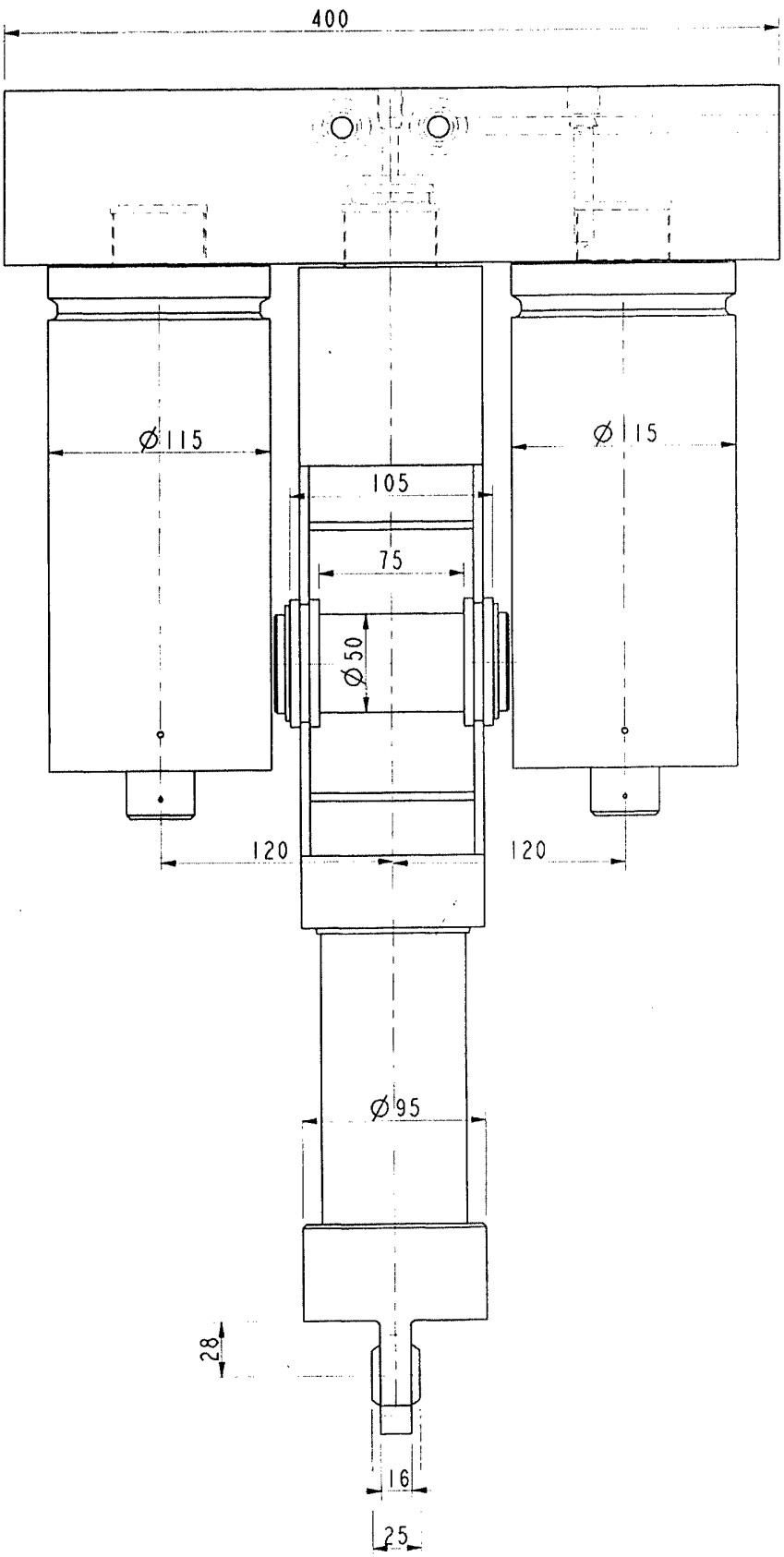
400
Ø115
Ø115
105
75
Ø50
120
120
Ø95
28
16
25

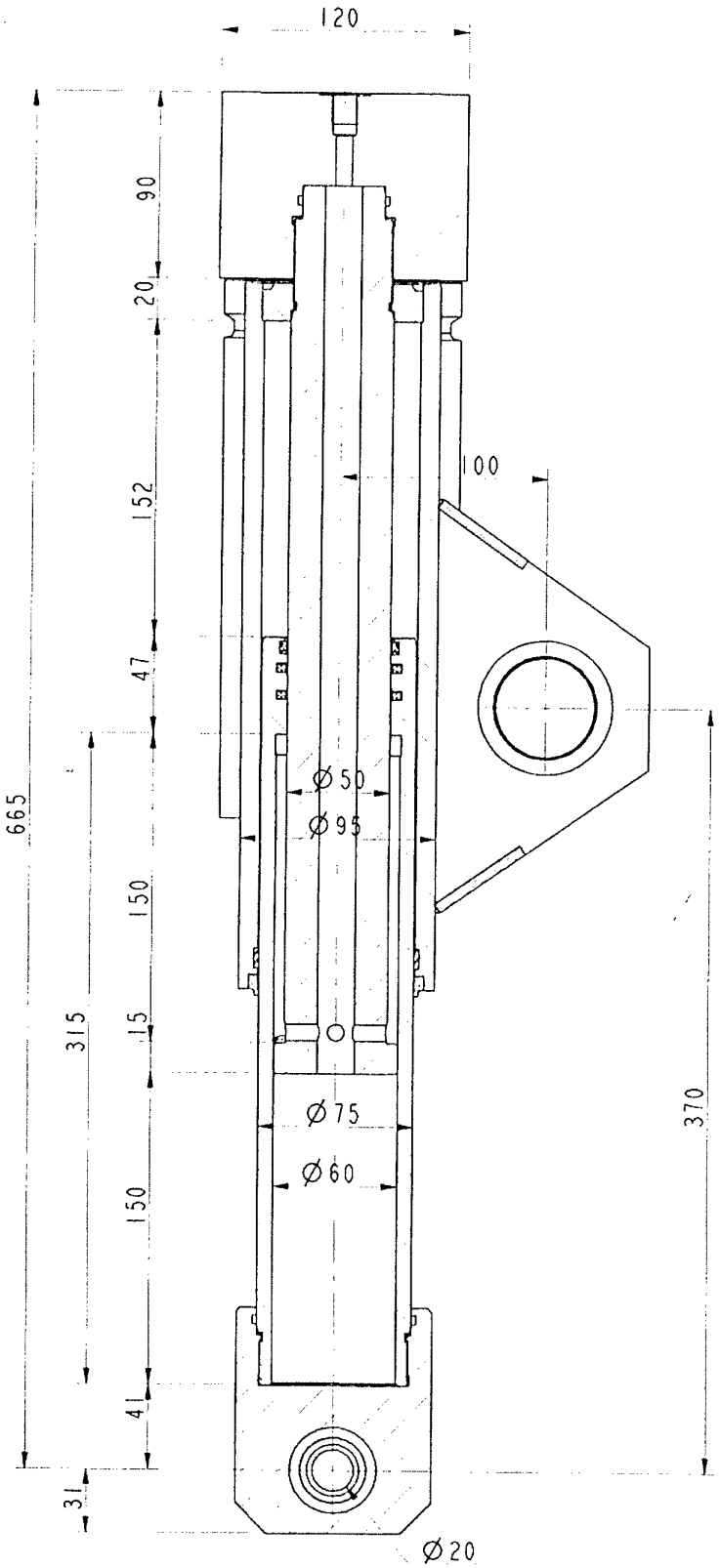
120
90
20
152
47
665
315
150
15
150
41
31
100
Ø50
Ø95
Ø75
Ø60
370
Ø20